

***N*-O-Isopropyl Sulfonamido-Based Hydroxamates: Design, Synthesis and Biological Evaluation of Selective Matrix Metalloproteinase-13 Inhibitors as Potential Therapeutic Agents for Osteoarthritis**

Elisa Nuti,[†] Francesca Casalini,[†] Stanislava I. Avramova,[†] Salvatore Santamaria,[†] Giovanni Cercignani,[‡] Luciana Marinelli,[§] Valeria La Pietra,[§] Ettore Novellino,[§] Elisabetta Orlandini,[†] Susanna Nencetti,[†] Tiziano Tuccinardi,^{†,⊥} Adriano Martinelli,[†] Ngee-Han Lim,^{||} Robert Visse,^{||} Hideaki Nagase,^{||} and Armando Rossello^{*,†}

[†]Dipartimento di Scienze Farmaceutiche, Università di Pisa, via Bonanno 6, 56126 Pisa, Italy, [‡]Dipartimento di Biologia, Unità di Biochimica, Università di Pisa, Via San Zeno 51, 56127 Pisa, Italy, [§]Dipartimento di Chimica Farmaceutica e Tossicologica, Università di Napoli "Federico II", Via Domenico Montesano 49, 80131 Napoli, Italy, ^{||}Department of Matrix Biology, The Kennedy Institute of Rheumatology Division, Imperial College, London W6 8LH, United Kingdom, and [⊥]Sbarro Institute for Cancer Research and Molecular Medicine, Center for Biotechnology, College of Science and Technology, Temple University, Philadelphia, Pennsylvania 19122

Received March 2, 2009

Matrix metalloproteinase-13 (MMP-13) is a key enzyme implicated in the degradation of the extracellular matrix in osteoarthritis (OA). For this reason, MMP-13 synthetic inhibitors are being sought as potential therapeutic agents to prevent cartilage degradation and to halt the progression of OA. Herein, we report the synthesis and in vitro evaluation of a new series of selective MMP-13 inhibitors possessing an arylsulfonamidic scaffold. Among these potential inhibitors, a very promising compound was discovered exhibiting nanomolar activity for MMP-13 and was highly selective for this enzyme compared to MMP-1, -14, and TACE. This compound acted as a slow-binding inhibitor of MMP-13 and was demonstrated to be effective in an in vitro collagen assay and in a model of cartilage degradation. Furthermore, a docking study was conducted for this compound in order to investigate its binding interactions with MMP-13 and the reasons for its selectivity toward MMP-13 versus other MMPs.

1. Introduction

Osteoarthritis (OA⁴) is characterized by the destruction of articular cartilage, chronic joint pain, and inflammation, and it is estimated to affect about 20 million people in the United States alone. The destruction of articular cartilage is largely due to the elevated activities of proteolytic enzymes that degrade the extracellular matrix (ECM) within the cartilage, whose main constituents are aggrecan and type II collagen.^{1–3} Collagen is a triple helical protein that is resistant to most proteases but is efficiently recognized and degraded by collagenase 3, known as matrix metalloproteinase-13 (MMP-13). MMP-13 catalyzes the hydrolysis of type II collagen at a unique site resulting in 3/4- and 1/4-length polypeptide products. This enzyme belongs to a family of enzymes termed matrix metalloproteinases (MMPs), which are zinc-dependent endopeptidases involved in the remodeling of extracellular matrix proteins. These endopeptidases have important roles in development,

morphogenesis, bone remodeling, wound healing, and angiogenesis. Furthermore, the overexpression of MMPs is associated with several pathologies, including cancer-cell invasion and metastasis, the loss of cartilage in osteoarthritis, rheumatoid arthritis, cardiovascular diseases, chronic obstructive pulmonary disease, and periodontitis.⁴

In osteoarthritis, chondrocytes stimulated by inflammatory cytokines, injury, or mechanical stimuli produce many MMPs, the most important of which is MMP-13, which is considered the principal target in arthritis. MMP-13 is not found in normal adult tissues but is expressed in the joints and articular cartilage of osteoarthritis patients.⁵ Furthermore, a MMP inhibitor that preferentially inhibits MMP-13 has been shown to block the degradation of explanted human osteoarthritic cartilage.⁶ On the basis of these findings, MMP-13 synthetic inhibitors are being sought as potential therapeutic agents to prevent cartilage degradation and to slow down the progression of OA.³ Unfortunately, few MMP inhibitors (MMPi) have been examined in clinical trials for OA and none have been successfully utilized as therapeutic agents so far. In fact, many broad spectrum MMP inhibitors have been found to display a dose-limiting toxicity in the form of musculoskeletal side effects including joint stiffness and inflammation.⁷ Although the human joint side effects are reversible upon withdrawal of the drug, musculoskeletal syndrome (MSS) has halted clinical trials of many nonselective MMPi. While the inhibition of specific MMPs such as MMP-1 or MMP-14 has been postulated to be responsible for MSS, the exact cause of this pathology is not yet clear. Others have speculated that sheddase inhibition, specifically inhibition of tumor necrosis factor- α converting enzyme (TACE), could be

*To whom correspondence should be addressed. Phone: +39 050 2219562. Fax: +39 050 2219605. E-mail: aros@farm.unipi.it.

⁴ Abbreviations: OA, osteoarthritis; ECM, extracellular matrix; MMP, matrix metalloproteinase; MSS, musculoskeletal syndrome; TACE, tumor necrosis factor- α converting enzyme; MMPi, MMP inhibitor; ZBG, zinc-binding group; DIAD, diisopropyl azodicarboxylate; SDS-PAGE, sodium dodecyl sulfate-polyacrylamide gel electrophoresis; IL-1 α , interleukin-1 α ; GAG, glycosaminoglycan; ADAMTS, a disintegrin and metalloproteinase with thrombospondin type I repeats; Hypo, hydroxyproline; OSM, oncostatin M; PDB, protein data bank; TIMP, tissue inhibitor of metalloproteinase; EDC, *N*-(3-Dimethylaminopropyl)-*N*'-ethylcarbodiimide hydrochloride; APMA, *p*-aminophenylmercuric acetate; DMMB, dimethylmethylene blue; DMBA, dimethylaminobenzaldehyde; GALS, genetic algorithm local search; RESP, restrained electrostatic potential; rmsd, root-mean square deviation; SAR, structure–activity relationship.

responsible for the observed side effects. The underlying mechanisms may possibly be mediated through the failure to downregulate receptor signaling by proteolytic release of the extracellular domain.⁸ Therefore, trying to reduce the likelihood of MSS is an important therapeutic consideration when treating osteoarthritis. Hence, pharmaceutical research has mainly focused on the discovery of potent inhibitors of MMP-13 displaying a high degree of selectivity over other MMPs.^{9–12} Almost all MMPs are based on a chelating moiety interacting with a catalytic zinc ion and a hydrophobic portion protruding into the hydrophobic S1' subsite, which is a deep pocket situated in proximity to the catalytic zinc ion. These compounds behave as competitive inhibitors because the zinc-binding group (ZBG) binding mode can mimic one of the transition states occurring during the substrate hydrolysis.¹³ Widely utilized ZBGs include: hydroxamic acids, carboxylic acids, and thiols. The most used of these is the hydroxamate group because it has excellent chelating properties.

MMPs have been classified on the basis of their substrate specificity into the five following classes: gelatinases (MMP-2 and MMP-9), collagenases (MMP-1, -8, -13), stromelysins (MMP-3, -10), membrane types (MMP-14, -16, -17), and other related enzymes such as matrilysin (MMP-7).¹⁴ There is a shared similarity in the overall three-dimensional fold for the MMPs, which is consistent with the relatively high sequence homology (>40%), which makes the design of a selective MMPI a difficult task. The major structural difference observed between the MMP enzymes is the relative size and shape of the S1' pocket. This site is also the major

substrate determinant that has been exploited for designing selective inhibitors.¹⁵ For instance, non-zinc-chelating inhibitors that are highly selective for MMP-13 and that exclusively bind the S1' pocket have recently been reported.¹⁶

In the course of our research on sulfonylated MMP inhibitors, we have previously reported compound **1a**¹⁷ (Figure 1), which is an arylsulfonamido hydroxamic acid¹⁸ that showed good selectivity for MMP-2 over MMP-1 and MMP-14. Compound **1a** represented the first example of a new family of tertiary sulfonamides (the *N*-*O*-alkyl sulfonamides) possessing a small *O*-alkyl group on their sulfonamido nitrogen. This type of inhibitors resulted in highly selective inhibition for MMP-2, even with respect to other potent sulfonamido-based analogues that were later developed,¹⁹ belonging to the well-known family of *N*-alkyl tertiary sulfonamides. In an effort to shift the activity and selectivity toward MMP-13 as target for OA, we aimed to modify the arylsulfonyl moiety that interacts with the S1' subsite. The active-site structure of MMP-13 is well-known in the literature because many X-ray crystallography and NMR studies have been reported on complexes of this enzyme with different inhibitors.^{20–23} Bearing in mind that the MMP-13 S1' subsite is an unusually large and deep pocket, we designed a series of arylsulfonamido hydroxamates analogues of **1a** that incorporate bulky and long P1' substituents.

A comparison of the inhibitory activity of **1a** with those of previously reported 4'-biphenyl sulfonylated analogues (**2**¹⁷ and **3**²⁴) devoid of the oxygen atom linked to the sulfonamide moiety, which is present in **1a**, prompted us to maintain the *N*-*O*-isopropyl group in the new series of compounds. This substituent was demonstrated to be important in order to achieve selectivity over MMP-1 and MMP-14, and it minimally affected the activity on MMP-2 and MMP-13 (Table 1).

Therefore, in the present paper, we report the synthesis and preliminary biological evaluation of a new series of *N*-isopropoxy-arylsulfonamides, **4a–l** (Figure 1), bearing different aryl substituents on the sulfonamidic portion. These compounds were assayed in vitro using recombinant MMPs, and the most promising scaffold was modified by introducing an alkyl group in the α position relative to the hydroxamate in order to increase its inhibitory activity. Compound **5** (Figure 1) was found to be a potent and highly selective slow-binding inhibitor of MMP-13 in the enzymatic assay and was successively tested in vitro on collagen and cartilage explants. Finally, molecular modeling studies were performed with the aim of revealing, at an atomic level, the interactions

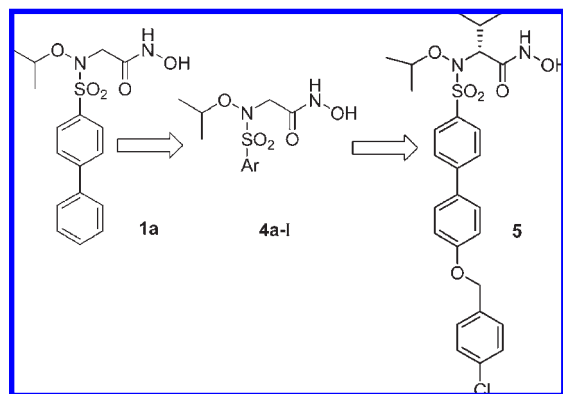
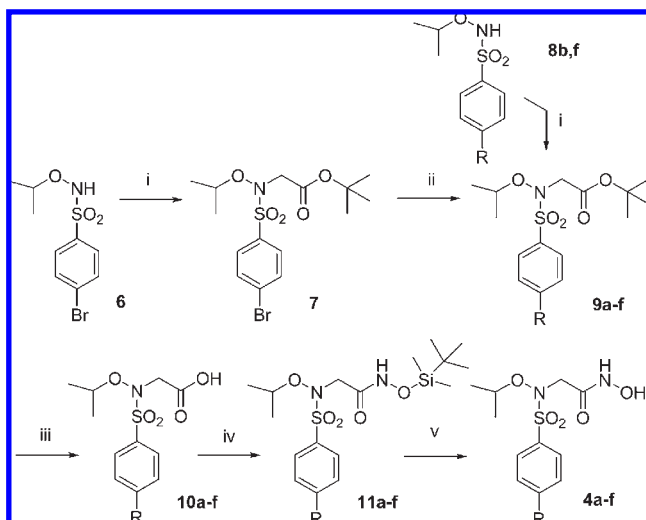


Figure 1. Progression of the SAR: from the lead compound **1a** to the MMP-13 selective inhibitor **5**.

Table 1. In Vitro^a Activity (IC₅₀ nM Values) of Biphenylsulfonamide Hydroxamic Acids **1a–3**

compd	R	MMP-1	MMP-2	MMP-3	MMP-8	MMP-9	MMP-13	MMP-14
1a	<i>O</i> - <i>i</i> -Pr	12000 ± 1000	12 ± 2	5900 ± 340	260 ± 10	200 ± 60	45 ± 2	2300 ± 170
2	<i>i</i> -Bu	4800 ± 300	12 ± 2	920 ± 50	48 ± 3	34 ± 2	39 ± 2	530 ± 40
3	H	610 ± 50	2.0 ± 0.2	320 ± 25	7.0 ± 0.7	34 ± 1	2.8 ± 0.3	70 ± 3

^a Assays were run in triplicate. The final values given here are the mean ± SD of three independent experiments.

Scheme 1. Synthesis of *N*-Isopropoxy-arylsulfonamide Hydroxamates **4a–f**^a

^a Reagents and conditions: (i) $\text{BrCH}_2\text{COO}t\text{-Bu}$, Cs_2CO_3 , $\text{Bu}_4\text{NH}\cdot\text{SO}_4$, DMF; (ii) $\text{RB}(\text{OH})_2$, $\text{Pd}(\text{PPh}_3)_4$, K_3PO_4 , dioxane/ H_2O , 70 °C; (iii) TFA, CH_2Cl_2 , 0 °C; (iv) TBDMSiONH_2 , EDC, CH_2Cl_2 ; (v) TFA, CH_2Cl_2 , 0 °C.

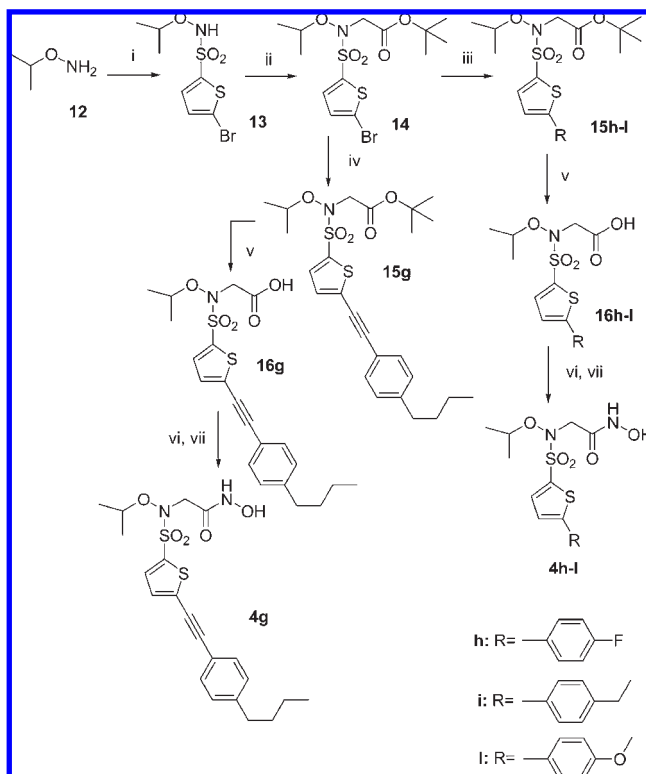
that govern the recognition and the binding of **5** to the target MMP-13. These findings are a prerequisite for understanding this compound's therapeutic activity toward OA as well as shedding light onto the structural features responsible for the lack of activity toward MMP-1, -14, and TACE.

2. Chemistry

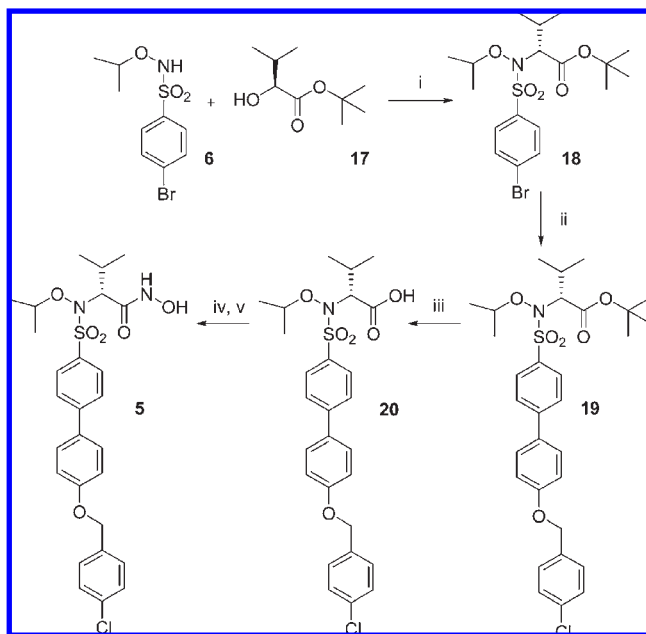
N-Isopropoxy-arylsulfonamide hydroxamates **4a–f** were prepared as described in Scheme 1. 4-Bromo-*N*-isopropoxybenzenesulfonamide **6**, synthesized as previously reported,²⁵ was reacted with *tert*-butyl bromoacetate in the presence of cesium carbonate to generate ester **7**. Similarly, sulfonamides **8b,f**²⁵ were converted to *tert*-butyl esters **9b,f**. Arylsulfonamide esters **9a,c–e** were obtained by Suzuki coupling of aryl bromide **7** with the appropriate arylboronic acid using $\text{Pd}(\text{PPh}_3)_4$ as the catalyst. Acid hydrolysis of esters **9a–f** yielded carboxylates **10a–f**, which were finally converted to their corresponding hydroxamates by condensation with *O*-(*tert*-butyldimethylsilyl)hydroxylamine and acid cleavage by TFA.²⁶

The thiophene derivatives **4g–I** were synthesized by following an analogous route, as reported in Scheme 2. Commercially available 5-bromothiophene-2-sulfonyl chloride (**12**)¹⁷ in THF, yielding 5-bromo-*N*-isopropoxythiophene-2-sulfonamide **13**, which was alkylated with *tert*-butyl bromoacetate to give ester **14**. This ester was successively converted by Suzuki coupling to *para*-fluoro, *para*-ethyl, and *para*-methoxy biaryl derivatives **15h–I**, which finally generated hydroxamates **4h–I**. The same 5-bromothiophene intermediate **14** was submitted to the Sonogashira reaction²⁷ in the presence of Pd(II), CuI, and triethylamine to produce the acetylenic derivative **15g**, which was converted into the corresponding hydroxamic acid **4g** as described above.

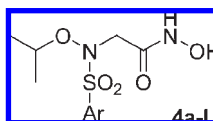
Optically active compound **5** (Scheme 3) was prepared starting from the (*S*)- α -hydroxy-*tert*-butyl-ester **17**, which was synthesized as previously described.²⁸ A Mitsunobu reaction of sulfonamide **6** with the alcohol **17** in the presence

Scheme 2. Synthesis of *N*-Isopropoxy-arylsulfonamide Hydroxamates **4g–I**^a

^a Reagents and conditions: (i) 5-bromothiophene-2-sulfonyl chloride, NMM, THF; (ii) $\text{BrCH}_2\text{COO}t\text{-Bu}$, Cs_2CO_3 , $\text{Bu}_4\text{NH}\cdot\text{SO}_4$, DMF; (iii) $\text{RB}(\text{OH})_2$, $\text{Pd}(\text{PPh}_3)_4$, K_3PO_4 , dioxane/ H_2O , 70 °C; (iv) 1-butyl-4-ethynyl benzene, $\text{Pd}(\text{PPh}_3)_2\text{Cl}_2$, CuI, TEA, DMF; (v) TFA, CH_2Cl_2 , 0 °C; (vi) TBDMSiONH_2 , EDC, CH_2Cl_2 ; (vii) TFA, CH_2Cl_2 , 0 °C.

Scheme 3. Preparation of Compound **5**^a

^a Reagents and conditions: (i) PPh_3 , DIAD, THF; (ii) 4-(4'-chloro-benzyloxy)-phenylboronic acid, $\text{Pd}(\text{PPh}_3)_4$, K_3PO_4 , dioxane/ H_2O , 70 °C; (iii) TFA, CH_2Cl_2 , 0 °C; (iv) TBDMSiONH_2 , EDC, CH_2Cl_2 ; (v) TFA, CH_2Cl_2 , 0 °C.

Table 2. In Vitro^a Activity (IC₅₀ nM Values) of *N*-Isopropoxy-arylsulfonamides, **4a–l**

Compd	Ar	MMP-1	MMP-2	MMP-3	MMP-8	MMP-9	MMP-13	MMP-14
4a		3300±300	1.5±0.1	1300±140	37±2	77±7	7.2±0.6	320±28
4b		13000±1900	4.2±0.3	1800±160	65±4	160±14	10±1	1000±100
4c		11000±1800	5.5±0.6	1600±230	560±54	44±3	15±1	5500±560
4d		13000±1100	40±3	1800±120	1700±100	1100±100	19±2	3400±360
4e		5600±270	74±5	710±99	3600±240	2300±140	41±4	2800±470
4f		59000±6300	26±3	1200±140	66±5	110±10	63±4	590±41
4g		13000±1000	360±23	4300±320	7600±480	4400±410	260±16	11000±1000
4h		20000±1900	310±17	9100±860	440±26	3200±230	600±54	6500±300
4i		>10000 ^b	56±4	4300±500	140±6	680±61	91±7	2400±230
4l		>10000 ^b	17±1	1200±140	110±10	250±16	25±3	>1000 ^b

^a Assays were run in triplicate. The final values given here are the mean ± SD of three independent experiments. ^b IC₅₀ values in the high micromolar range could not be accurately estimated due to fluorescence emission from the compound.

of diisopropyl azodicarboxylate (DIAD) and triphenylphosphine gave the *tert*-butyl ester (**R-18**). The aryl intermediate **18** was then converted into **19** by Pd-catalyzed Suzuki coupling with 4-(4'-chlorobenzoyloxy)-phenylboronic acid in the presence of K₃PO₄. Acid cleavage of **19** yielded the carboxylic acid **20**, which was finally converted to its corresponding hydroxamate **5** by condensation with *O*-(*tert*-butyldimethylsilyl)hydroxylamine, followed by acid hydrolysis with TFA.

3. Results and Discussion

MMP Inhibition. The new hydroxamic acids synthesized (**4a–l** and **5**) were tested in vitro on human recombinant MMPs by a fluorometric assay, which used a fluorogenic peptide²⁹ as the substrate. Results are reported in Tables 2 and 3, together with those already obtained for the previously described analogues **1a–3** (Table 1).

As can be seen from data in Table 2, changing from a biphenyl (as in compound **1a**) to a 4-substituted biphenyl group in P1' (as in **4a–c**) caused a general increase in the inhibitory activity of all tested enzymes without affecting the selectivity profile. In fact, these derivatives were better inhibitors for MMP-2 than for MMP-13, although they remained poor inhibitors for MMP-1 and -14. In particular, the methylthio derivative **4a** was the most active inhibitor for

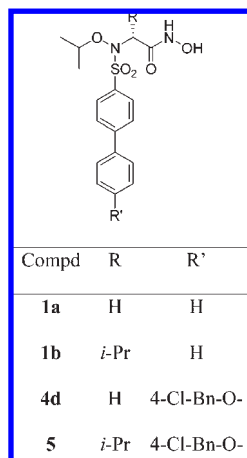
MMP-13 with an IC₅₀ = 7.2 nM. The introduction of a phenoxybenzenesulfonyl substituent (as in compound **4f**) caused a decrease in inhibitory activity for MMP-13 and MMP-2 relative to **1a**, which was accompanied by a subsequent decrease in selectivity. The replacement of a benzene ring with a 2,5-disubstituted thiophene ring in the sulfonyl group, as in the **4g–l** derivatives, led to a reduction of activity against MMP-13 and MMP-2 while only slightly affecting the inhibitory activity on MMP-1 and MMP-14. This reduction in inhibitory activity was probably due to a loss in linearity of the arylsulfonyl moiety, which adversely affected the binding affinity for the S1' pocket.

The best results were observed for derivatives **4d,e**, which allowed the curved portion in the arylsulfonyl moiety to better fit with MMP-13 than with MMP-2. In fact, it is well-known from the literature that the main difference in the S1' pocket between MMP-13 and MMP-2 is that the MMP-2 S1' loop is two amino acids shorter.⁹ In MMP-2, the absence of residues analogous to G248 and S250 causes the loop to be displaced by 4 Å proximal to S250 of MMP-13. For this reason, the S1' pocket of MMP-13 was probably more suitable than that of MMP-2 to accommodate the curved-shaped arylsulfonyl moiety of **4d,e**. In particular, compound **4d** appeared to be the best of the series with a

Table 3. In Vitro^a Inhibitory Activity (IC₅₀ nM Values) of Compound **5** Compared to Those of the Previously Described Compounds **1a**, **1b**, and **4d**

compd	MMP-1	MMP-2	MMP-3	MMP-8	MMP-9	MMP-13	MMP-14	MMP-16	TACE
1a	12000 ± 1000	12 ± 2	5900 ± 340	260 ± 10	200 ± 60	45 ± 2	2300 ± 170	900 ± 48	> 100000
1b	490 ± 76	0.80 ± 0.20	50 ± 2	1.6 ± 0.1	6.7 ± 1.6	4.1 ± 0.2	9.8 ± 0.2	51 ± 3	14000 ± 1000
4d	13000 ± 1100	40 ± 3	1800 ± 120	1700 ± 100	1100 ± 100	19 ± 2	3400 ± 360	15000 ± 1200	35000 ± 3400
5	48000 ± 2800	9.6 ± 0.4	180 ± 13	63 ± 3	69 ± 10	3.0 ± 0.2	14000 ± 1300	5000 ± 440	> 100000

^a Assays were run in triplicate. The final values given here are the mean ± SD of three independent experiments.

Chart 1

nanomolar activity for MMP-13 (IC₅₀ = 19 nM). This compound exhibited a slight selectivity over MMP-2 (IC₅₀ = 40 nM), a 1000-fold selectivity over MMP-1 and 200-fold selectivity over MMP-14. In addition, this derivative showed good selectivity for MMP-13 over MMP-3, -16, and TACE (all IC₅₀s were in the micromolar range) (Table 3).

On the basis of these results and in order to increase its inhibitory potency, we decided to further modify **4d** by introducing an alkyl substituent in position α of the hydroxamate. In fact, the introduction of an isopropyl group of the (*R*) configuration had already yielded good results when applied to the scaffold of compound **1a**, thereby leading to the discovery of compound **1b** (Chart 1) that was very active against MMP-2.^{28,30} Therefore, derivative **5**, bearing the same arylsulfonyl moiety of **4d** and an isopropyl group in P1, was synthesized to verify this hypothesis.

As expected, compound **5** (Table 3) proved to be the best of the series exhibiting a 6-fold increase in inhibitory potency against MMP-13 (IC₅₀ = 3.0 nM) and a lower activity for MMP-1, MMP-14, and TACE relative to **4d**. In addition, **5** displayed a 16000-fold selectivity for MMP-13 over MMP-1, a 5000-fold selectivity over MMP-14, and no measurable inhibitory activity toward TACE (IC₅₀ > 100 μ M). As shown in Table 3, compound **5** was more selective than **1a** and **1b** (in fact, the last was highly potent against MMP-2 but quite unselective for the other tested enzymes).

Slow-Binding Inhibition Assays. For the most active compound of the series, **5**, and its analogue devoid of the α -substituent, **4d**, a kinetic characterization was carried out in comparison with the 4-methoxybiphenyl derivative **4b** and with the biphenyl analogues **1a** and **1b**. To evaluate the kinetics of inhibition toward MMP-13 and MMP-2, an assay suited for the kinetic characterization of slow-binding inhibitors was used.³¹ The enzyme was added to a solution of fluorogenic substrate and increasing concentrations of the inhibitor. Slow-binding behavior was observed for **5**, **4d**, and **1b** with both

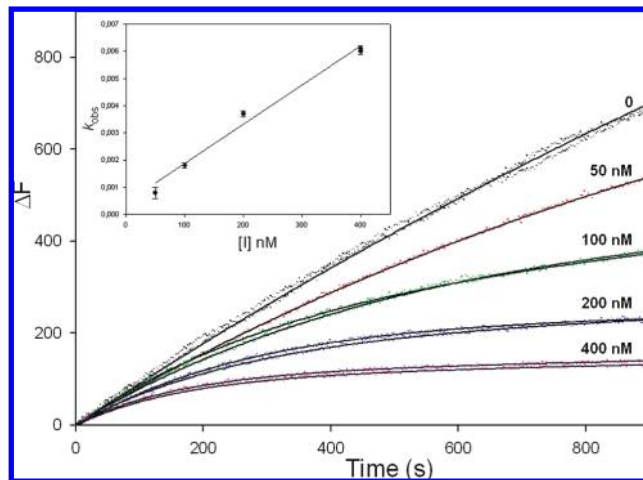


Figure 2. Progress curves relative to MMP-13 inhibition by compound **5**, in the first phase (15 min) after mixing, at four different concentrations in duplicate. Two control reaction mixtures (without inhibitor) are also shown. Dots represent fluorescence readings, continuous lines are best fits to the kinetic model of Duggleby.³² Inset: plot of k_{obs} vs $[I]$ used to calculate k_{on} and k_{off} .

enzymes. Figure 2 shows the reaction progress curves in the absence and presence of inhibitor **5** for MMP-13 inhibition.

In the absence of inhibitor, the steady-state rate of hydrolysis of the fluorogenic substrate was reached immediately and the reaction progress curve was essentially linear. In addition, straight lines were also observed in the presence of fast-binding inhibitors. However, in the presence of a slow-binding inhibitor, there was a slow decrease in reaction rate, which varied as a function of the inhibitor concentration. Depending on the inhibitor, different concentration ranges had to be used in order to obtain experimental progress curves that could be analyzed according to Duggleby³² (see Experimental Section). Nevertheless, preincubation of the enzyme with the inhibitor for an appropriate period of time (4 h) gave rise to linear reaction courses (final steady-state rates). The K_i values of the slow-binding component for inhibition against **5**, **4d**, and **1b** are listed in Table 4.

Compounds **4b** and **1a** did not show slow-binding behavior for either MMP-13 or MMP-2. Thus, their K_i values were determined from the slopes of the progress curves because k_{on} and k_{off} values could not be evaluated under our assay conditions. The slow-binding behavior of compounds **5**, **4d**, and **1b** (k_{on} of the order 10^4 – 10^5 $\text{M}^{-1}\text{s}^{-1}$) were matched by nanomolar range K_i values due to comparatively low values for the offset rate constants (k_{off} of the order 10^{-4} – 10^{-3} s^{-1}).

Taking into account the results shown in Table 4, it could be suggested that the presence of a P1 substituent (the isopropyl group of the (*R*) configuration) might be responsible for the slow-binding behavior of the inhibitor. However, a bent and extended P1' substituent, such as the *p*-chlorobenzoyloxy moiety present in **4d** and **5**, probably contributed to this property. In fact, the α -unsubstituted

Table 4. Kinetic Parameters^a for Compounds **5**, **4b,d**, and **1a,b** Calculated for Inhibition of MMP-13 and MMP-2

compd	MMP-13				MMP-2			
	$k_{\text{off}} \times 10^{-4} (\text{s}^{-1})$	$k_{\text{on}} \times 10^4 (\text{M}^{-1}\text{s}^{-1})$	$K_i (\text{nM})$	r^2	$k_{\text{off}} \times 10^{-4} (\text{s}^{-1})$	$k_{\text{on}} \times 10^4 (\text{M}^{-1}\text{s}^{-1})$	$K_i (\text{nM})$	r^2
5	4.0 ± 3.0	1.4 ± 0.1	29 ± 1	0.9794	6.0 ± 3.0	1.1 ± 0.1	54 ± 2	0.9707
4d	6.0 ± 2.0	7.3 ± 0.3	8.2 ± 0.3	0.9875	22 ± 7	8.7 ± 1.0	25 ± 1	0.8805
4b	N/A ^b	N/A	5.8 ± 0.2	N/A	N/A ^b	N/A	3.8 ± 0.2	N/A
1a	N/A ^b	N/A	20 ± 1	N/A	N/A ^b	N/A	13 ± 2	N/A
1b	6.0 ± 3.0	40 ± 2	1.5 ± 0.5	0.9756	3.3 ± 2.0	33 ± 2	1.0 ± 0.1	0.9634

^aThe kinetic parameters were evaluated as described in the Experimental Section. ^bN/A, not applicable (no slow-binding behavior).

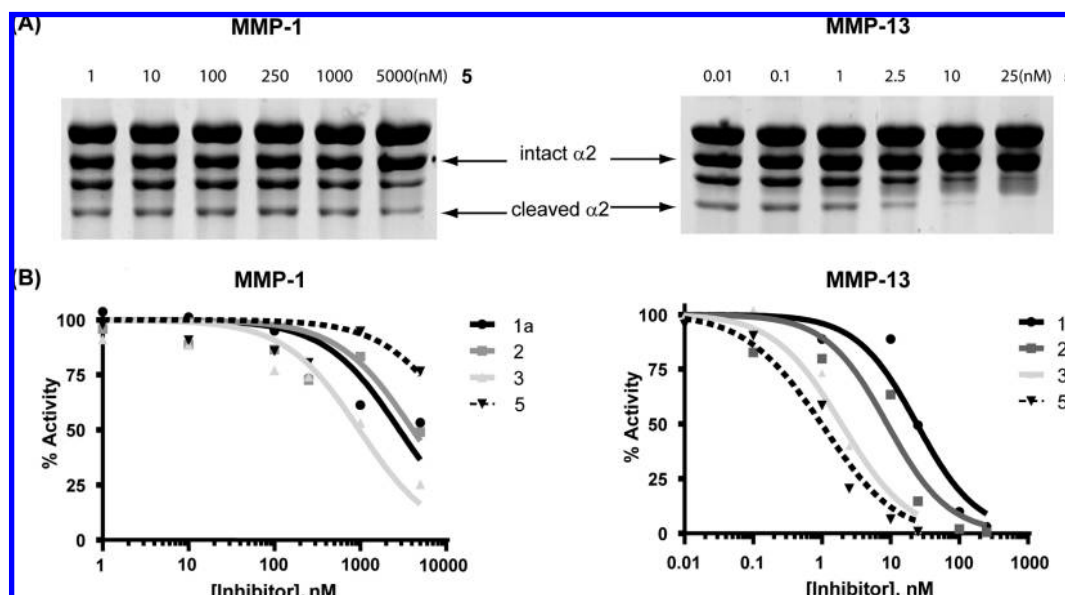


Figure 3. Effect of inhibitors on collagen degradation by MMP-1 and MMP-13. (A) SDS-PAGE analysis of the reactions for the effect of **5** on MMP-1 (left) and MMP-13 (right) cleavage of collagen, with arrows indicating the intact and cleaved collagen $\alpha 2$ chain used for densitometric analysis. (B) Graphs representing the remaining % activity of the MMPs after incubation with the various inhibitors **1a** (black closed circles, solid line), **2** (dark-gray squares, solid line), **3** (light-gray triangles, solid line), and **5** (black triangles, dotted line).

derivative **4d** also showed a slow-binding behavior. The lowest association constant (k_{on}) for inhibition against MMP-13 was measured for compound **5**, which bears both of these moieties. The difference in association constants was 5-fold between **5** and **4d** and 30-fold between **5** and **1b**. Moreover, compound **5** exhibited the slowest dissociation constant (k_{off}). The slow dissociation rate of this compound would predictably result in a long duration of action and, consequently, it would not be necessary to maintain high systemic levels of drug to continuously inhibit the target enzyme. Importantly, no relevant difference in the slow-binding kinetic constants between MMP-2 and MMP-13 was observed.

Collagenase Assays. Having identified compound **5** with a high affinity and promising selectivity for MMP-13, the activity of this analogue on MMP-13 and MMP-1 was assessed by a collagenase assay in comparison to the previously described compounds **1a–3**. IC_{50} s were determined against full-length MMP-1 and MMP-13 with type I collagen as a substrate. Samples were run on sodium dodecyl sulfate polyacrylamide gel electrophoresis (SDS-PAGE), and the amount of collagen cleavage was determined by densitometry (Figure 3).

The IC_{50} values obtained for collagen were in agreement with those obtained using the peptide substrate (Table 5), with **5** being the worst inhibitor for MMP-1 and the best for MMP-13.

Cartilage Degradation Assays. Compound **5** and its progenitor **1a** were also tested in a porcine articular cartilage

Table 5. In Vitro Activity (IC_{50} , nM) of **1a–3** and **5** by Collagenase Assay

compd	MMP-1 (collagen) ^a	MMP-13 (collagen) ^a
1a	2900 ± 1100	25 ± 4
2	4100 ± 1600	9.4 ± 0.2
3	970 ± 290	2.4 ± 0.1
5	15000 ± 8200	1.4 ± 0.2

^aCollagen was used as substrate.

explant model in order to verify the activity of these inhibitors on collagen and aggrecan degradation occurring during osteoarthritis. The explants were cultured under the stimuli of interleukin-1 α (IL-1 α) and oncostatin M (OSM), which cause aggrecan degradation for the first 7–10 days and then collagen degradation after approximately 20 days.³³ As reported in Figure 4A, the inhibitors were not effective at blocking aggrecan breakdown, represented by glycosaminoglycan (GAG) release, at any of the doses tested. These data indicate that these compounds were probably not active against the aggrecanases, members of the disintegrin and metalloproteinase with thrombospondin type I repeats (ADAMTS) family, which are the enzymes considered to be responsible for aggrecan degradation.³⁴

In contrast, collagen degradation measured by hydroxyproline (Hypro) release was inhibited in a concentration-dependent manner by both inhibitors, with **1a** being less effective than **5** (Figure 4B). Compound **1a** was only effective

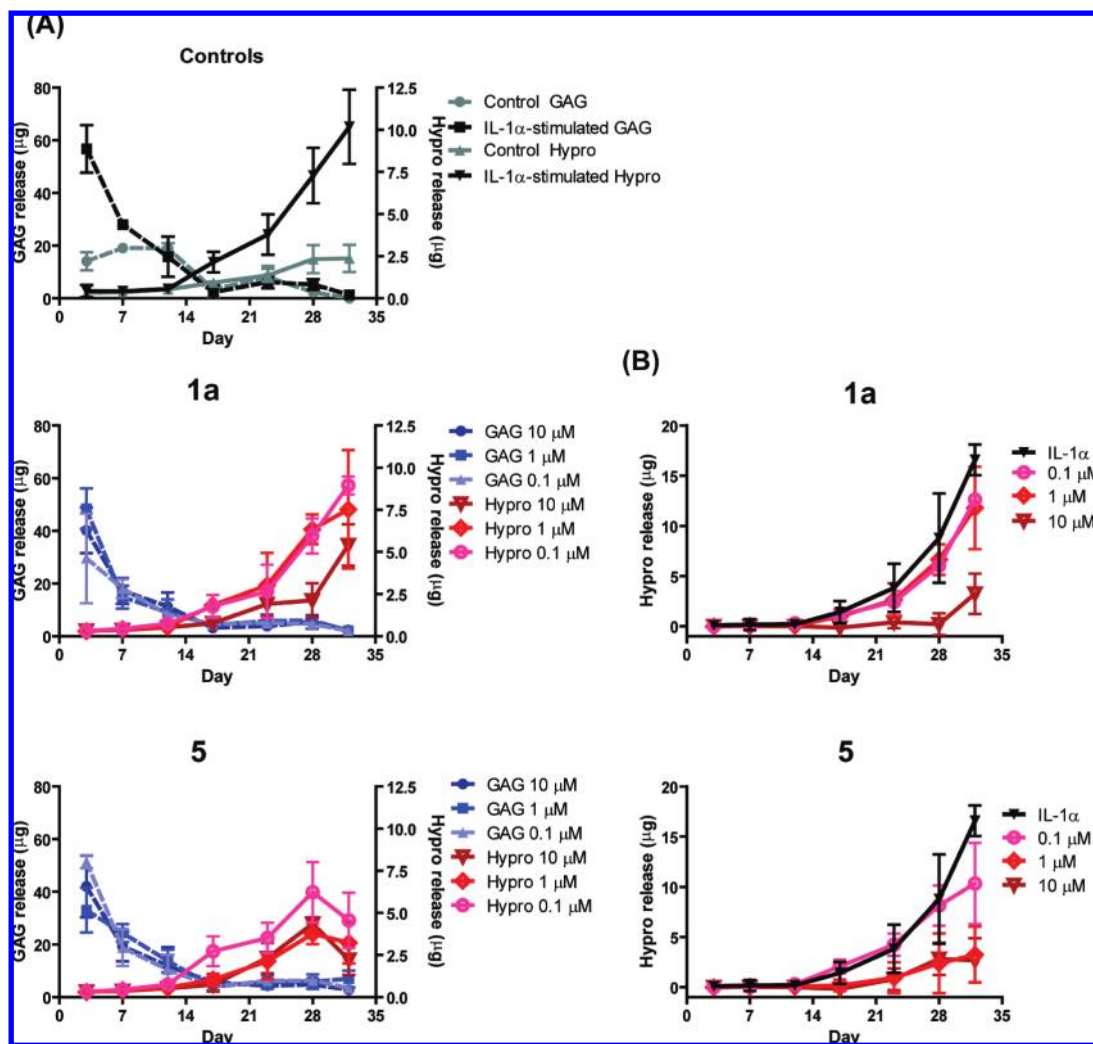


Figure 4. Effect of inhibitors on aggrecan and collagen degradation in long-term IL-1 α -stimulated porcine articular cartilage explants cultures. Cartilage was stimulated with IL-1 α (10 ng/mL) in the presence or absence of the inhibitor compounds **1a** and **5** at various concentrations (0.1, 1, and 10 μ M). The medium was replenished every 3 or 4 days. (A) The amount of GAG (dashed lines) and Hypro (solid lines) released into each medium was determined in the control (top), compound **1a** treated (middle), and compound **5** treated (bottom) cartilage. (B) The cumulative amount of Hypro released into the medium with the background release of Hypro (without stimulation) subtracted of compound **1a** (top) and compound **5** (bottom) treated cartilage.

in blocking collagen degradation at 10 μ M, whereas **5** was effective at 1 μ M. This finding very roughly corresponds to the fact that **5** was a 10-fold better inhibitor for MMP-13 than **1a** in both the fluorometric and in the collagenase assay. Hence, in the IL-1 α /OSM stimulated model of cartilage degradation, it appeared that the enzyme responsible for collagenolysis was MMP-13, as compound **5** was highly selective for that enzyme.

4. Molecular Modeling

Molecular modeling was performed with the aim of revealing, at an atomic level, the potential interactions that govern the recognition and the binding of **5** to MMP-13 as well as shedding light on the structural features responsible for the apparent inactivity toward MMP-1, -14, and TACE. In the attempt to overcome the rigidity of the enzymes during the ligand docking process, a detailed comparison among the X-ray structures currently available was performed for each MMP, and those that were most diverse were selected for docking experiments. Obviously, this approach does not ensure representation of all energetically accessible conformations of MMPs or conforma-

tional changes, which may occur upon binding of our particular ligand. However, this strategy did allow the exploitation of the crystallographic data collected to date on MMPs.

X-ray Structures Selection for Docking Studies. As for the MMP-1 X-ray structures, an apo form (PDB code: 1SU3³⁵), a full length form (PDB code: 2CLT³⁶), a form bound to TIMP-1 (PDB code: 2J0T³⁷), and three forms that were complexed to organic inhibitors (PDB code: 1HFC,³⁸ 2TCL,³⁹ 966C²⁰) have been reported in the RCSB Protein Data Bank (PDB). A superposition on the α carbon atoms and using 1HFC as the reference indicated that the protein folding was highly preserved. However, in 966C, the R214 side chain was displaced from its lowest energy position upon inhibitor binding, thereby opening the S1' pocket. Thus, the 1HFC, where the S1' was closed, and the 966C, where it was open, were both selected for ligand docking studies.

Thirteen MMP-13 X-ray structures have been released in the PDB. Besides that cocrystallized with TIMP-2, all the others were cocrystallized with organic inhibitors such as the 4-[4-(4-chloro-phenoxy)-benzenesulfonylmethyl]-tetrahydropyran-4-carboxylic acid hydroxyamide⁴⁰ (RS-130830) (PDB

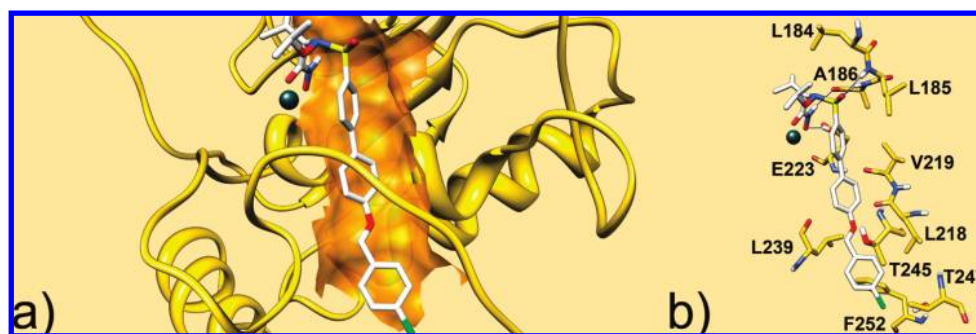


Figure 5. Docked structure of **5** into the MMP-13, where a portion of the binding site is visible as gold surface (left side). Detailed interaction mode of **5** with MMP-13 active site residues (right side). H-Bonds are displayed as gray lines.

code: 830C²⁰). A superposition of all X-ray structures on the α carbon atoms using 830C as the reference structure showed that the protein folding and the shape of the catalytic loops were highly superimposable. In addition, the large majority of the residues were all preserved in the side chain conformations in the catalytic site. Thus, in this case, only 830C with the lower resolution (1.60 Å) was selected for our docking studies.

Several TACE X-ray structures are available cocrystallized with TIMP-3 as well as with peptidic or organic inhibitors. A superposition, performed as before with the other MMPs, revealed a strict conservation of the protein folding and noteworthy flexibility of the S1' specificity loop. Thus, the three structures (3E8R,⁴¹ 2I47,⁴² 2OIO⁴³) that were the most divergent in the S1' loop shape were considered for docking of compound **5**.

With regard to the MMP-14 X-ray structures, we used 1BUV because only two identical structures, complexed with TIMP-2, were available in the PDB (1BUV, 1BQQ).⁴⁴

Docking of 5 on MMP-13. In the lowest energy docked conformation of **5**, the hydroxamic acid moiety coordinated the catalytic zinc atom in a bidentate fashion with the two oxygen atoms and established two hydrogen bonds with the carbonyl oxygen of A186 and with the E223 side chain.

The *N*-*O*-isopropyl sulfonamide group was in a conformation in which the N-lone pair bisected the O=S=O angle. According to search results from the Cambridge Structural Databases, this conformation was the most common one in the case of acyclic N–O sulfonamides.

The *N*-*O*-isopropyl group of **5** was between L184 and I243 side chains with which hydrophobic interactions were formed (the distances between the isopropyl central carbon and the L184 and L185 C γ were 6.7 and 6.6 Å, respectively). Furthermore, other lipophilic contacts were detectable between the isopropyl group bound to the inhibitor's C α and the L184 side chain.

From these docking results, it is clear that the sulfonamide moiety was particularly important. This group formed a bifurcated hydrogen bond with L185 and the A186 backbone amine, thereby enabling the *p*-Cl-benzyloxy-diphenyl moiety to plunge deep into the unusually large S1'-specificity pocket (Figure 5). In the S1', the *p*-Cl-benzyl ring of **5** established a chlorine-reinforced T-shaped interaction with the aromatic ring of F252 and formed hydrophobic interactions with L218 and L239 side chains and with hydrophobic portions of T245 and T247. In **5**, the phenyl ring next to the sulfonamide group was flanked by lipophilic residues such as L185 and V219. Clearly, all these interactions endowed **5** with a low nanomolar inhibitory activity toward MMP-13.

Docking of 5 on MMP-1, -14, and TACE. Currently, there are only two well-defined structures of MMP-1 available in the PDB. These forms mainly differ in the S1' pocket, which can be in a "closed" (low energy) or in an "open" (inhibitor induced) conformation. Specifically, upon binding of the *N*-hydroxy-2-[4-(4-phenoxy-benzenesulfonyl)-tetrahydro-pyran-4-yl]-acetamide (RS-104966),⁴⁰ multiple residue side chains (e.g., L181, R214, V215, S239, Y240, and F242) change in their conformation. In particular, the R214 side chain was demonstrated to be forced to adopt a new position, which enlarged the S1' pocket.²⁰ Docking of **5** in the "open" conformation of MMP-1 revealed a binding mode perfectly superimposable to that obtained for MMP-13 when a high inhibitory activity was found. However, two interactions between MMP-13 and **5** at residues F252 and L184 are lost in MMP-1 that has V246 and N180, respectively. Nevertheless, the loss of these two interactions does not fully explain the experimentally observed poor inhibition of MMP-1 by **5** (IC₅₀ = 48.3 μ M). It is possible that **5** was not able to induce the "open" conformational change observed upon RS-104966 binding. Thus, docking calculations in the MMP-1 "closed" conformation were also performed. In the lowest energy binding position, **5** was positioned in a way that the metal ion was coordinated by its hydroxamate moiety and the isopropyl group was partially inserted in the S1' pocket. Thus, the hydrophobic contacts were still visible, but the remainder of **5** was largely solvent exposed. Notably, the aromatic branch of **5** was too long to insert into the closed conformation of the S1' pocket. In light of the experimental data, the results obtained using MMP-1 in the "closed" conformation appear more reasonable.

In regard to the low activity of **5** toward MMP-14, only two out of 100 docked conformations showed the occurrence of metal coordination and occupancy of the S1' pocket at the same time. However, a careful inspection of the binding mode revealed that in order to fit into the narrow S1' pocket, the biphenyl moiety must have adopted a deeply unfavorable geometry where the torsion between the two rings was 90° (Car1-Car1-Car2-Car2). Thus, the low activity of **5** toward MMP-14 can be mainly attributed to the variations in the S1' pockets. Indeed, although MMP-13 and -14 possess a S1' specificity loop of the same length, the latter has a narrower shaped S1' pocket. The partially closed fold of the S1' specificity loop in MMP-14 seems to be because the sV-hB connecting loop, which is immediately below the S1' specificity loop, is three amino acids longer. Moreover, the sequence identity between the two S1' specificity loops is rather low (25%) and the substitution of T245 and T247 in MMP-13 with Q262 and M264 in MMP-14 leads to a further

restriction of the S1' channel. This comparative analysis once more strengthens the concept that the differential substitutions of the S1' pocket can be successfully used to design selective inhibitors. Another remarkable difference between MMP-13 and -14, which could have affected our ligand binding process and could be corroborated by the SARs herein developed, resides in the sIII-sIV connecting loop. In this instance, (MMP-13)-L184 is substituted by (MMP-14)-F198 and this effectively reduces the available room in the S1 pocket. Notably, only the membrane-type MMP-14 and -16 contain a Phe residue at this position, while the following smaller amino acids are present in other MMPs: N (MMP-1), L (MMP-2, -9, -13), I (MMP-8, -11, -12), V (MMP-3), T (MMP-7), and S (MMP-10). Thus, these described structural variations of MMP-14 can be taken into account in the fine-tuning of a specific inhibitor's activity.

The docking of **5** into the three most divergent TACE X-ray structures furnishes a clear explanation of the structural features responsible for the observed inactivity against this enzyme. In fact, despite the substantial structural similarities in the active sites between TACE and MMP-13, the unique shape of the S1' specificity pocket of TACE does not allow the full occupancy by the long and semirigid P1' substituent of **5** and the simultaneous metal coordination by the hydroxamate moiety. Indeed, it is well established^{45,46} that TACE inhibitors must have a bent shaped P1' group in order to properly adapt to the curved contour of the TACE S1' tunnel.

Although the molecular modeling studies presented herein surely provide valuable explanations for the ligand activity and selectivity, X-ray crystallography would be needed to finally prove these predictions.

5. Conclusions

A new series of *N*-isopropoxy-arylsulfonamide inhibitors for MMP-13, selective over MMP-1 and MMP-14, was designed and synthesized by optimizing the structural characteristics of the previously described derivative **1a**. Among the novel analogues, a very promising compound was discovered (**5**), which showed nanomolar activity for MMP-13 and high selectivity over MMP-1, -14, -16, and TACE. A kinetic characterization of **5** showed a slow-binding behavior of this inhibitor toward MMP-13 and MMP-2. The slow dissociation of this compound would predictably result in a long duration of action and, consequently, it would not be necessary to maintain high systemic levels of drug to continuously inhibit the target enzyme. Because of its promising properties, **5** was chosen for further studies examining collagen degradation that confirmed the data obtained with isolated enzymes by a fluorometric assay. Finally, hydroxamates **5** and **1a** were assayed in the IL-1 α /OSM stimulated model of cartilage degradation, and both compounds showed no significant effect on aggrecan degradation, thereby suggesting to be inactive toward aggrecanases. The inhibitory activity of **5** on cartilage breakdown was 10-fold better than **1a**, which very roughly corresponded to the fact that **5** was a 10-fold better inhibitor for MMP-13 than **1a**. Thus, on the basis of the effectiveness of the MMP-13 selective inhibitor **5**, it can be deduced that the major collagenase involved in the IL-1 α stimulated porcine cartilage degradation model is probably MMP-13.

The next steps of our research program will be the evaluation of the *in vivo* efficacy of **5** in OA models and a further

optimization of its selectivity profile. In this respect, it is not clear whether the dual specificity of compound **5** for MMP-13 and MMP-2 will be beneficial or not in terms of protecting cartilage degradation. In fact, the role of MMP-2 activity itself in the pathogenesis of OA is unclear. Interestingly, mRNA levels of MMP-2 are increased in OA patients compared to normal controls, suggesting that MMP-2 may play a negative role in this disease.⁴⁷ On the other hand, MMP-2-null mice exhibit a more severe arthritic phenotype than wild type mice in antigen-induced arthritis, suggesting that the total loss of MMP-2 activity is unfavorable.⁴⁸ Further modifying compound **5** to reduce MMP-2-cross reactivity will bypass these concerns.

6. Experimental Section

Chemistry. Melting points were determined on a Kofler hot-stage apparatus and are uncorrected. ¹H and ¹³C NMR spectra were determined with a Varian Gemini 200 MHz spectrometer. Chemical shifts (δ) are reported in parts per million downfield from tetramethylsilane and referenced from solvent references. Coupling constants *J* are reported in hertz; ¹³C NMR spectra were fully decoupled. The following abbreviations are used: singlet (s), doublet (d), triplet (t), double-doublet (dd), broad (br), and multiplet (m). Where indicated, the elemental compositions of the compounds agreed to within $\pm 0.4\%$ of the calculated value. Chromatographic separations were performed on silica gel columns by flash column chromatography (Kieselgel 40, 0.040–0.063 mm; Merck) or using ISOLUTE Flash Si II cartridges (STEPBIO). Reactions were followed by thin-layer chromatography (TLC) on Merck aluminum silica gel (60 F254) sheets that were visualized under a UV lamp, and hydroxamic acids were visualized with FeCl₃ aqueous solution. Evaporation was performed *in vacuo* (rotating evaporator). Sodium sulfate was always used as the drying agent. Commercially available chemicals were purchased from Sigma-Aldrich. The purity of the final compounds was determined by reverse-phase HPLC on a Merck Hitachi D-7000 liquid chromatograph. HPLC purity was determined to be >95% for all final products using a Discovery C18 column (250 mm \times 4.6 mm, 5 μ m, Supelco), with a gradient of 20% water/80% methanol at a flow rate of 1.4 mL/min, with UV monitoring at the fixed wavelength of 256 nm. See the Supporting Information for compound purity analysis data for final compounds. Optical rotation were obtained on a Perkin-Elmer 343 polarimeter with a continuous Na lamp (589 nm).

tert-Butyl 2-(4-Bromo-*N*-isopropoxyphenylsulfonamido)acetate (7). A solution of sulfonamide **6** (2.0 g, 6.8 mmol) in anhydrous DMF (14.4 mL) was treated with *tert*-butyl bromoacetate (1.2 mL, 8.16 mmol), cesium carbonate (2.2 g, 6.8 mmol), and tetrabutylammonium hydrogen sulfate (2.3 g, 6.8 mmol). The reaction mixture was stirred for 3 days at room temperature, diluted with H₂O, and extracted with EtOAc. The combined organic extracts were dried over anhydrous Na₂SO₄, filtered, and evaporated under reduced pressure to afford **7** as a white solid (2.68 g, 96.4% yield); mp 89–90 °C. ¹H NMR (CDCl₃) δ : 1.24 (d, *J* = 6.4 Hz, 6H), 1.45 (s, 9H), 3.58 (br s, 2H), 4.53 (septet, *J* = 6.2 Hz, 1H), 7.67–7.76 (m, 4H).

General Procedure for the Preparation of esters 9a,c–e. A solution of aryl bromide **7** (500 mg, 1.22 mmol) in anhydrous dioxane (12.2 mL)/H₂O (2.7 mL) was sequentially treated under nitrogen with K₃PO₄ (596.5 mg, 2.81 mmol), the appropriate arylboronic acid (2.00 mmol), and Pd(PPh₃)₄ (141 mg, 0.12 mmol). The resulting mixture was stirred for 20 min at 70 °C. After being cooled to RT, the mixture was treated with NaHCO₃ and extracted with EtOAc. The combined organic extracts were dried over anhydrous Na₂SO₄, filtered, and evaporated under reduced pressure. The crude was purified by flash chromatography on silica gel column.

tert-Butyl 2-(*N*-isopropoxy-4'-(methylthio)biphenyl-4-ylsulfonamido)acetate (9a). The title compound was prepared from aryl bromide **7** and 4-(methylthio)phenylboronic acid following the general procedure. Purified with *n*-hexane/EtOAc 7:1 (25%) as white solid; mp 115–116 °C. ¹H NMR (CDCl₃) δ: 1.26 (d, *J* = 6.4 Hz, 6H), 1.46 (s, 9H), 2.53 (s, 3H), 3.63 (br s, 2H), 4.58 (septet, *J* = 6.2 Hz, 1H), 7.32–7.36 (m, 2H), 7.53–7.56 (m, 2H), 7.71–7.75 (m, 2H), 7.89–7.93 (m, 2H).

tert-Butyl 2-(4'-Butoxy-*N*-isopropoxybiphenyl-4-ylsulfonamido)acetate (9c). The title compound was prepared from aryl bromide **7** and 4-butoxyphenylboronic acid following the general procedure. Purified with *n*-hexane/EtOAc 10:1 (25%) as a colorless oil. ¹H NMR (CDCl₃) δ: 0.99 (t, *J* = 7.3 Hz, 3H), 1.26 (d, *J* = 6.2 Hz, 6H), 1.42–1.53 (m, 11H), 1.73–1.87 (m, 2H), 3.62 (br s, 2H), 4.02 (t, *J* = 6.6 Hz, 2H), 4.58 (septet, *J* = 6.2 Hz, 1H), 6.97–7.02 (m, 2H), 7.53–7.57 (m, 2H), 7.69–7.73 (m, 2H), 7.87–7.91 (m, 2H).

tert-Butyl 2-(4'-(4-Chlorobenzyloxy)-*N*-isopropoxybiphenyl-4-ylsulfonamido)acetate (9d). The title compound was prepared from aryl bromide **7** and 4-(4-chlorobenzyloxy)phenylboronic acid following the general procedure. Purified with *n*-hexane/EtOAc 5:1 (25%) as a solid. ¹H NMR (CDCl₃) δ: 1.26 (d, *J* = 6.2 Hz, 6H), 1.46 (s, 9H), 3.63 (br s, 2H), 4.58 (septet, *J* = 6.0 Hz, 1H), 5.09 (s, 2H), 7.03–7.08 (m, 2H), 7.38 (s, 4H), 7.54–7.59 (m, 2H), 7.69–7.73 (m, 2H), 7.87–7.92 (m, 2H).

(*E*)-tert-Butyl 2-(4-(2-(Biphenyl-4-yl)vinyl)-*N*-isopropoxyphenylsulfonamido)acetate (9e). The title compound was prepared from aryl bromide **7** and (*E*)-2-(biphenyl-4-yl)vinylboronic acid following the general procedure. Purified with *n*-hexane/EtOAc 9:1 (25%) as a yellow solid. ¹H NMR (CDCl₃) δ: 1.25 (d, *J* = 6.2 Hz, 6H), 1.47 (s, 9H), 3.61 (br s, 2H), 4.56 (septet, *J* = 6.2 Hz, 1H), 7.20 (s, 1H), 7.34–7.50 (m, 5H), 7.61–7.70 (m, 7H), 7.83–7.87 (m, 2H).

General Procedure for the Preparation of Esters 9b,f. A solution of sulfonamide **8b** or **8f** (0.62 mmol) in anhydrous DMF (1.3 mL) was treated with *tert*-butyl bromoacetate (0.11 mL, 0.74 mmol), cesium carbonate (202 mg, 0.62 mmol), and tetrabutylammonium hydrogen sulfate (210.5 mg, 0.62 mmol). The reaction mixture was stirred for 3 days at room temperature, diluted with H₂O, and extracted three times with EtOAc. The combined organic extracts were dried over anhydrous Na₂SO₄, filtered, and evaporated under reduced pressure to afford **9b** and **9f**. The crude products were purified by flash chromatography.

tert-Butyl 2-(*N*-isopropoxy-4'-methoxybiphenyl-4-ylsulfonamido)acetate (9b). The title compound was prepared from sulfonamide **8b** following the general procedure. Purified with *n*-hexane/EtOAc 8:1 using a ISOLUTE FLASH Si II cartridge (STEPBIO) (66%) as a white solid. ¹H NMR (CDCl₃) δ: 1.26 (d, *J* = 6.2 Hz, 6H), 1.46 (s, 9H), 3.62 (br s, 2H), 3.87 (s, 3H), 4.58 (septet, *J* = 6.2 Hz, 1H), 6.97–7.05 (m, 2H), 7.53–7.61 (m, 2H), 7.69–7.73 (m, 2H), 7.87–7.92 (m, 2H).

tert-Butyl 2-(*N*-isopropoxy-4-phenoxyphenylsulfonamido)acetate (9f). The title compound was prepared from sulfonamide **8f** following the general procedure. Purified with *n*-hexane/EtOAc 15:1 (45%) as a yellow oil. ¹H NMR (CDCl₃) δ: 1.23 (d, *J* = 6.2 Hz, 6H), 1.46 (s, 9H), 3.59 (br s, 2H), 4.55 (septet, *J* = 6.2 Hz, 1H), 7.03–7.12 (m, 4H), 7.24–7.27 (m, 1H), 7.39–7.47 (m, 2H), 7.76–7.82 (m, 2H).

General Procedure for the Preparation of Carboxylic Acids 10a–f. TFA (14.82 mmol, 1.14 mL) was added dropwise to a stirred, ice-chilled solution of *tert*-butyl esters **9a–f** (0.26 mmol) in freshly distilled dichloromethane (2.0 mL). The mixture was stirred under these reaction conditions for 5 h, and the solvent was removed in vacuo to give the carboxylic acids **10a–f**. The crude products were purified by trituration with *n*-hexane/Et₂O.

2-(*N*-isopropoxy-4'-(methylthio)biphenyl-4-ylsulfonamido)acetic Acid (10a). The title compound was prepared from ester **9a** following the general procedure. White solid (98% yield); mp 116–117 °C. ¹H NMR (CDCl₃) δ: 1.27 (d, *J* = 6.2 Hz,

6H), 2.54 (s, 3H), 3.81 (br s, 2H), 4.57 (septet, *J* = 6.2 Hz, 1H), 7.33–7.37 (m, 2H), 7.53–7.58 (m, 2H), 7.73–7.77 (m, 2H), 7.90–7.95 (m, 2H).

2-(*N*-isopropoxy-4'-methoxybiphenyl-4-ylsulfonamido)acetic Acid (10b). The title compound was prepared from ester **9b** following the general procedure. White solid (77% yield); mp 110–111 °C. ¹H NMR (CDCl₃) δ: 1.26 (d, *J* = 6.2 Hz, 6H), 3.82 (br s, 2H), 3.87 (s, 3H), 4.57 (septet, *J* = 6.2 Hz, 1H), 6.99–7.04 (m, 2H), 7.55–7.60 (m, 2H), 7.71–7.75 (m, 2H), 7.88–7.93 (m, 2H).

2-(4'-Butoxy-*N*-isopropoxybiphenyl-4-ylsulfonamido)acetic Acid (10c). The title compound was prepared from ester **9c** following the general procedure. White solid (79% yield); mp 79–80 °C. ¹H NMR (CDCl₃) δ: 0.99 (t, *J* = 7.3 Hz, 3H), 1.25 (d, *J* = 6.2 Hz, 6H), 1.41–1.61 (m, 2H), 1.73–1.85 (m, 2H), 3.81 (br s, 2H), 4.02 (t, *J* = 6.4 Hz, 2H), 4.57 (septet, *J* = 6.4 Hz, 1H), 6.98–7.02 (m, 2H), 7.54–7.58 (m, 2H), 7.71–7.75 (m, 2H), 7.88–7.92 (m, 2H).

2-(4'-(4-Chlorobenzyloxy)-*N*-isopropoxybiphenyl-4-ylsulfonamido)acetic Acid (10d). The title compound was prepared from ester **9d** following the general procedure. Yellow oil (88% yield). ¹H NMR (DMSO-*d*₆) δ: 1.17 (d, *J* = 6.2 Hz, 6H), 3.67 (s, 2H), 4.41 (septet, *J* = 6.4 Hz, 1H), 5.19 (s, 2H), 7.13–7.17 (m, 2H), 7.48 (s, 4H), 7.73–7.77 (m, 2H), 7.85–7.91 (m, 4H).

(*E*)-2-(4-(2-(Biphenyl-4-yl)vinyl)-*N*-isopropoxyphenylsulfonamido)acetic Acid (10e). The title compound was prepared from ester **9e** following the general procedure. Solid (70% yield); mp 185–186 °C. ¹H NMR (DMSO-*d*₆) δ: 1.17 (d, *J* = 6.2 Hz, 6H), 3.66 (s, 2H), 4.40 (septet, *J* = 6.2 Hz, 1H), 7.34–7.54 (m, 5H), 7.71–7.75 (m, 6H), 7.82–7.94 (m, 4H).

2-(*N*-isopropoxy-4-phenoxyphenylsulfonamido)acetic Acid (10f). The title compound was prepared from ester **9f** following the general procedure. Pale yellow oil (90% yield). ¹H NMR (CDCl₃) δ: 1.23 (d, *J* = 5.6 Hz, 6H), 3.77 (s, 2H), 4.27 (br s, 1H), 4.54 (septet, *J* = 6.2 Hz, 1H), 7.05–7.12 (m, 4H), 7.21–7.29 (m, 1H), 7.40–7.47 (m, 2H), 7.79–7.83 (m, 2H).

General Procedure for the Preparation of *O*-TBDMS Acid Hydroxyamides (11a–f). 1-[3-(Dimethylamino)propyl]-3-ethyl carbodiimide hydrochloride (EDC) was added portionwise (34.5 mg, 0.18 mmol) to a stirred and cooled solution (0 °C) of the appropriate carboxylic acid **10a–f** (0.12 mmol), and *O*-(*tert*-butyldimethylsilyl)hydroxylamine (17.7 mg, 0.12 mmol) in freshly distilled CH₂Cl₂ (2.5 mL). After stirring at room temperature overnight, the mixture was washed with water and the organic phase was dried and evaporated in vacuo to afford the *O*-silylate intermediates **11a–f**.

***N*-(*tert*-butyldimethylsilyloxy)-2-(*N*-isopropoxy-4'-(methylthio)-biphenyl-4-ylsulfonamido)acetamide (11a).** The title compound was prepared from carboxylic acid **10a** following the general procedure. The crude product was purified by flash chromatography with *n*-hexane/EtOAc 6:1 using a ISOLUTE FLASH Si II cartridge (STEPBIO). White solid (26% yield). ¹H NMR (CDCl₃) δ: 0.21 (s, 6H), 0.97 (s, 9H), 1.25 (d, *J* = 6.2 Hz, 6H), 2.53 (s, 3H), 3.71 (br s, 2H), 4.47 (septet, *J* = 6.2 Hz, 1H), 7.32–7.37 (m, 2H), 7.53–7.57 (m, 2H), 7.73–7.77 (m, 2H), 7.89–7.93 (m, 2H), 8.60 (br s, 2H).

***N*-(*tert*-butyldimethylsilyloxy)-2-(*N*-isopropoxy-4'-methoxybiphenyl-4-ylsulfonamido)acetamide (11b).** The title compound was prepared from carboxylic acid **10b** following the general procedure. The crude product was purified by flash chromatography with *n*-hexane/EtOAc 4:1 using a ISOLUTE FLASH Si II cartridge (STEPBIO). White solid (64% yield). ¹H NMR (CDCl₃) δ: 0.21 (s, 6H), 0.97 (s, 9H), 1.26 (d, *J* = 6.2 Hz, 6H), 3.71 (br s, 2H), 3.87 (s, 3H), 4.46 (septet, *J* = 6.2 Hz, 1H), 6.99–7.04 (m, 2H), 7.55–7.59 (m, 2H), 7.71–7.75 (m, 2H), 7.88–7.92 (m, 2H), 8.57 (br s, 1H).

2-(4'-Butoxy-*N*-isopropoxybiphenyl-4-ylsulfonamido)-*N*-(*tert*-butyldimethylsilyloxy)acetamide (11c). The title compound was prepared from carboxylic acid **10c** following the general procedure. The crude product was purified by flash chromatography on silica gel column (*n*-hexane/EtOAc 4:1). Colorless oil (25% yield). ¹H NMR (CDCl₃) δ: 0.21 (s, 6H), 0.91–1.02 (m, 12H), 1.25 (d, *J* = 5.6 Hz,

6H), 1.45–1.57 (m, 2H), 1.73–1.83 (m, 2H), 3.71 (s, 2H), 4.02 (t, $J = 6.6$ Hz, 2H), 4.45 (septet, $J = 5.6$ Hz, 1H), 6.98–7.02 (m, 2H), 7.53–7.57 (m, 2H), 7.71–7.75 (m, 2H), 7.87–7.91 (m, 2H), 8.57 (br s, 1H).

***N*-(*tert*-Butyldimethylsilyloxy)-2-(4'-(4-chlorobenzoyloxy)-*N*-isopropoxybiphenyl-4-ylsulfonamido)acetamide (11d).** The title compound was prepared from carboxylic acid **10d** following the general procedure. The crude product was purified by flash chromatography on silica gel column (*n*-hexane/EtOAc 3:1). Yellow oil (25% yield). ^1H NMR (CDCl_3) δ : 0.21 (s, 6H), 0.97 (s, 9H), 1.26 (d, $J = 6.2$ Hz, 6H), 3.71 (s, 2H), 4.46 (septet, $J = 6.2$ Hz, 1H), 5.09 (s, 2H), 7.04–7.08 (m, 2H), 7.38 (s, 4H), 7.54–7.59 (m, 2H), 7.71–7.75 (m, 2H), 7.88–7.92 (m, 2H), 8.56 (br s, 1H).

(*E*)-2-(4-(2-(Biphenyl-4-yl)vinyl)-*N*-isopropoxyphenylsulfonamido)-*N*-(*tert*-butyldimethylsilyloxy)acetamide (11e). The title compound was prepared from carboxylic acid **10e** following the general procedure. The crude product was purified by flash chromatography on silica gel column (*n*-hexane/EtOAc 3.5:1). Yellow solid (35% yield). ^1H NMR (CDCl_3) δ : 0.22 (s, 6H), 0.98 (s, 9H), 1.25 (d, $J = 6.0$ Hz, 6H), 3.72 (s, 2H), 4.45 (septet, $J = 6.2$ Hz, 1H), 7.20 (s, 1H), 7.28 (s, 1H), 7.36–7.50 (m, 4H), 7.61–7.72 (m, 7H), 7.83–7.88 (m, 2H), 8.56 (br s, 1H).

***N*-(*tert*-Butyldimethylsilyloxy)-2-(*N*-isopropoxy-4-phenoxyphenylsulfonamido)acetamide (11f).** The title compound was prepared from carboxylic acid **10f** following the general procedure. The crude product was purified by flash chromatography on silica gel column (*n*-hexane/EtOAc 4:1). White solid (25% yield); mp 131–132 °C. ^1H NMR (CDCl_3) δ : 0.21 (s, 6H), 0.98 (s, 9H), 1.24 (d, $J = 5.6$ Hz, 6H), 3.67 (s, 2H), 4.43 (septet, $J = 6.0$ Hz, 1H), 7.05–7.11 (m, 4H), 7.21–7.28 (m, 1H), 7.40–7.50 (m, 2H), 7.78–7.82 (m, 2H), 8.56 (br s, 1H).

General Procedure to Synthesize Hydroxamic Acids 4a–f. TFA (0.31 mL, 3.99 mmol) was added dropwise to a stirred and ice-chilled solution of the appropriate *O*-silylate **11a–f** (0.07 mmol) in CH_2Cl_2 (0.5 mL). The solution was stirred under these reaction conditions for 5 h, and the solvent was removed in vacuo. The crude products were purified by trituration with *n*-hexane/ Et_2O .

***N*-hydroxy-2-(*N*-isopropoxy-4'-(methylthio)biphenyl-4-ylsulfonamido)acetamide (4a).** The title compound was prepared from *O*-silylate intermediate **11a** following the general procedure. White solid (95% yield); mp 134–135 °C. ^1H NMR (CDCl_3) δ : 1.25 (d, $J = 6.2$ Hz, 6H), 2.53 (s, 3H), 3.79 (s, 2H), 4.48 (septet, $J = 6.0$ Hz, 1H), 7.33–7.37 (m, 2H), 7.53–7.57 (m, 2H), 7.73–7.78 (m, 2H), 7.89–7.94 (m, 2H). ^{13}C NMR (CDCl_3) δ : 15.63, 21.33, 80.23, 126.74, 127.37, 127.76, 130.40, 135.33, 140.27, 146.87. Anal. ($\text{C}_{18}\text{H}_{22}\text{N}_2\text{O}_5\text{S}_2$) C, H, N.

***N*-Hydroxy-2-(*N*-isopropoxy-4'-methoxybiphenyl-4-ylsulfonamido)acetamide (4b).** The title compound was prepared from *O*-silylate intermediate **11b** following the general procedure. Solid (97% yield); mp 141–142 °C. ^1H NMR ($\text{DMSO}-d_6$) δ : 1.15 (d, $J = 6.2$ Hz, 6H), 3.82 (s, 3H), 4.34 (septet, $J = 6.2$ Hz, 1H), 7.06–7.10 (m, 2H), 7.73–7.77 (m, 2H), 7.86–7.97 (m, 4H), 10.71 (s, 1H). ^{13}C NMR ($\text{DMSO}-d_6$) δ : 20.91, 55.28, 78.39, 114.59, 126.57, 128.39, 129.99, 130.12, 130.21, 145.30, 159.89. Anal. ($\text{C}_{18}\text{H}_{22}\text{N}_2\text{O}_6\text{S}$) C, H, N.

2-(4'-Butoxy-*N*-isopropoxybiphenyl-4-ylsulfonamido)-*N*-hydroxyacetamide (4c). The title compound was prepared from *O*-silylate intermediate **11c** following the general procedure. Yellow solid (78% yield); mp 73–74 °C. ^1H NMR (CDCl_3) δ : 0.99 (t, $J = 7.5$ Hz, 3H), 1.25 (br s, 6H), 1.41–1.60 (m, 2H), 1.73–1.87 (m, 2H), 3.80 (br s, 2H), 4.01 (t, $J = 6.4$ Hz, 2H), 4.46 (br s, 1H), 6.97–7.02 (m, 2H), 7.53–7.57 (m, 2H), 7.68–7.75 (m, 2H), 7.87–7.93 (m, 2H). ^{13}C NMR (CDCl_3) δ : 14.05, 19.44, 21.31, 31.43, 68.01, 80.20, 115.23, 127.14, 128.63, 129.69, 130.32, 130.98, 147.26. Anal. ($\text{C}_{21}\text{H}_{28}\text{N}_2\text{O}_6\text{S}$) C, H, N.

2-(4'-(4-Chlorobenzoyloxy)-*N*-isopropoxybiphenyl-4-ylsulfonamido)-*N*-hydroxyacetamide (4d). The title compound was prepared from *O*-silylate intermediate **11d** following the general procedure. Yellow solid (78% yield); mp 88–89 °C. ^1H NMR (CDCl_3) δ : 1.26 (d, $J = 6.0$ Hz, 6H), 3.83 (s, 2H), 4.47

(septet, $J = 5.8$ Hz, 1H), 5.10 (s, 2H), 7.04–7.09 (m, 2H), 7.39 (s, 4H), 7.55–7.59 (m, 2H), 7.72–7.76 (m, 2H), 7.88–7.92 (m, 2H). ^{13}C NMR (CDCl_3) δ : 21.27, 69.51, 80.29, 115.61, 127.28, 128.78, 128.89, 128.98, 129.76, 130.36, 131.69, 134.07, 135.15, 147.17, 159.38. Anal. ($\text{C}_{24}\text{H}_{25}\text{ClN}_2\text{O}_6\text{S}$) C, H, N.

(*E*)-2-(4-(2-(Biphenyl-4-yl)vinyl)-*N*-isopropoxyphenylsulfonamido)-*N*-hydroxyacetamide (4e). The title compound was prepared from *O*-silylate intermediate **11e** following the general procedure. White solid (73% yield). ^1H NMR (CDCl_3) δ : 1.25 (d, $J = 5.8$ Hz, 6H), 3.80 (s, 2H), 4.46 (septet, $J = 6.2$ Hz, 1H), 7.20 (s, 1H), 7.28 (s, 1H), 7.36–7.49 (m, 4H), 7.63–7.72 (m, 7H), 7.84–7.88 (m, 2H). ^{13}C NMR [$(\text{CD}_3)_2\text{CO}$] δ : 21.39, 56.26, 79.67, 127.50, 128.03, 128.41, 129.71, 131.13, 131.97, 133.04, 135.84, 136.66, 141.03, 141.78, 144.15. Anal. ($\text{C}_{25}\text{H}_{26}\text{N}_2\text{O}_5\text{S}$) C, H, N.

***N*-Hydroxy-2-(*N*-isopropoxy-4-phenoxyphenylsulfonamido)acetamide (4f).** The title compound was prepared from *O*-silylate intermediate **11f** following the general procedure. Pale-yellow solid (75% yield); mp 112–113 °C. ^1H NMR (CDCl_3) δ : 1.22 (d, $J = 5.8$ Hz, 6H), 3.74 (s, 2H), 4.44 (m, 1H), 7.05–7.11 (m, 4H), 7.21–7.28 (m, 1H), 7.39–7.47 (m, 2H), 7.78–7.82 (m, 2H). ^{13}C NMR [$(\text{CD}_3)_2\text{CO}$] δ : 21.66, 79.96, 118.20, 121.62, 126.38, 131.49, 133.37, 156.02, 163.90. Anal. ($\text{C}_{17}\text{H}_{20}\text{N}_2\text{O}_6\text{S}$) C, H, N.

5-Bromo-*N*-isopropoxythiophene-2-sulfonamide (13). A solution of 5-bromothiophene-2-sulfonyl chloride (2.0 g, 8.9 mmol) in anhydrous THF (20 mL) was added dropwise to a stirred and cooled (0 °C) solution of *O*-isopropylhydroxylamine hydrochloride **12** (1.0 g, 8.9 mmol) and *N*-methylmorpholine (1.9 mL, 17.9 mmol) in anhydrous THF (20 mL). After stirring at rt for 4 days, the reaction mixture was diluted with EtOAc and washed with H_2O . The organic phase was dried over anhydrous Na_2SO_4 , filtered, and evaporated under reduced pressure to afford **13** as a yellow solid (2.17 g, 80.7% yield); mp 118–119 °C. ^1H NMR (CDCl_3) δ : 1.24 (d, $J = 6.2$ Hz, 6H), 4.31 (septet, $J = 6.0$, 1H), 6.80 (s, 1H), 7.12 (d, $J = 3.8$ Hz, 1H), 7.46 (d, $J = 4.0$ Hz, 1H).

***tert*-Butyl 2-(5-Bromo-*N*-isopropoxythiophene-2-sulfonamido)acetate (14).** A solution of sulfonamide **13** (1.0 g, 3.4 mmol) in anhydrous DMF (7.2 mL) was treated with *tert*-butyl bromoacetate (0.6 mL, 4.08 mmol), cesium carbonate (1.1 g, 3.4 mmol), and tetrabutylammonium hydrogen sulfate (1.15 g, 3.4 mmol). The reaction mixture was stirred for 3 days at room temperature, diluted with H_2O , and extracted with EtOAc. The combined organic extracts were dried over anhydrous Na_2SO_4 , filtered, and evaporated under reduced pressure. The crude product was purified by flash chromatography (*n*-hexane/ EtOAc 30:1) using a ISOLUTE FLASH Si II cartridge (STEPBIO) to afford **14** as a yellow solid (1.13 g, 79.4% yield). ^1H NMR (CDCl_3) δ : 1.27 (d, $J = 6.4$ Hz, 6H), 1.47 (s, 9H), 3.63 (br s, 2H), 4.56 (septet, $J = 6.2$ Hz, 1H), 7.14 (d, $J = 3.4$ Hz, 1H), 7.41 (d, $J = 3.4$ Hz, 1H).

***tert*-Butyl 2-(5-(4-Butylphenyl)ethynyl)-*N*-isopropoxythiophene-2-sulfonamido)acetate (15g).** To a solution of **14** (500 mg, 1.21 mmol) in 4.3 mL of DMF were added 1-butyl-4-ethynylbenzene (0.25 mL, 1.45 mmol), copper(I) iodide (11.5 mg, 0.06 mmol), dichlorobis(triphenylphosphine)palladium(II) (21 mg, 0.03 mmol), and triethylamine (0.34 mL, 2.42 mmol) at room temperature. The mixture was degassed and stirred under an argon atmosphere at rt for 30 min. The mixture was poured into water and extracted with EtOAc. The organic solution was washed with 1 N HCl, 5% NaHCO_3 solution, and brine, dried, and evaporated. The residue was purified by flash chromatography (*n*-hexane/EtOAc 30:1) using a ISOLUTE FLASH Si II cartridge (STEPBIO) to give **15g** as a yellow oil (26% yield). ^1H NMR (CDCl_3) δ : 0.93 (t, $J = 6.9$ Hz, 3H), 1.28 (d, $J = 6.2$ Hz, 6H), 1.33–1.41 (m, 2H), 1.47 (s, 9H), 1.53–1.68 (m, 2H), 2.63 (t, $J = 7.8$ Hz, 2H), 3.66 (br s, 2H), 4.59 (septet, $J = 6.2$ Hz, 1H), 7.17–7.23 (m, 3H), 7.42–7.46 (m, 2H), 7.55 (d, $J = 4.0$ Hz, 1H).

2-(5-(4-Butylphenyl)ethynyl)-*N*-isopropoxythiophene-2-sulfonamido)acetic Acid (16g). TFA (0.9 mL, 11.74 mmol) was added dropwise to a stirred, ice-chilled solution of *tert*-butyl ester **15g**

(101.1 mg, 0.21 mmol) in freshly distilled dichloromethane (1.6 mL). The mixture was stirred under these reaction conditions for 5 h, and the solvent was removed in vacuo. The crude product was purified by trituration with *n*-hexane/Et₂O to give **16g** as a yellow solid (90 mg, 95% yield). ¹H NMR (CDCl₃) δ: 0.92 (t, *J* = 7.1 Hz, 3H), 1.24–1.40 (m, 8H), 1.54–1.66 (m, 2H), 2.62 (t, *J* = 7.3 Hz, 2H), 3.94 (s, 2H), 4.50 (septet, *J* = 6.4 Hz, 1H), 7.16–7.20 (m, 3H), 7.40–7.44 (m, 2H), 7.49 (d, *J* = 3.4 Hz, 1H).

2-(5-((4-Butylphenyl)ethynyl)-*N*-isopropoxythiophene-2-sulfonamido)-*N*-hydroxyacetamide (4g). 1-[3-(Dimethylamino)propyl]-3-ethyl carbodiimide hydrochloride (EDC) was added portionwise (60.4 mg, 0.31 mmol) to a stirred and cooled solution (0 °C) of the carboxylic acid **16g** (92.4 mg, 0.21 mmol) and *O*-(*tert*-butyldimethylsilyl)hydroxylamine (30.9 mg, 0.21 mmol) in freshly distilled CH₂Cl₂ (4.5 mL). After stirring at room temperature overnight, the mixture was washed with water and the organic phase was dried and evaporated in vacuo. The crude was purified by flash chromatography on silica gel (*n*-hexane/EtOAc 4:1) to afford the *O*-silylate intermediate. ¹H NMR (CDCl₃) δ: 0.21 (s, 6H), 0.89–0.92 (m, 3H), 0.97 (s, 9H), 1.27 (d, *J* = 6.2 Hz, 6H), 1.33–1.40 (m, 2H), 1.53–1.67 (m, 2H), 2.63 (t, *J* = 7.8 Hz, 2H), 3.74 (s, 2H), 4.48 (septet, *J* = 6.4 Hz, 1H), 7.17–7.24 (m, 3H), 7.42–7.46 (m, 2H), 7.57 (d, *J* = 4.0 Hz, 1H), 8.45 (br s, 1H).

TFA (0.2 mL, 2.85 mmol) was added dropwise to a stirred and ice-chilled solution of *O*-silylate (26 mg, 0.05 mmol) in CH₂Cl₂ (0.5 mL). The solution was stirred under these reaction conditions for 5 h, and the solvent was removed in vacuo. The crude product was purified by trituration with *n*-hexane/Et₂O to give the hydroxamate **4g** as a solid (16 mg, 71% yield); mp 66–67 °C. ¹H NMR [(CD₃)₂CO] δ: 0.92 (t, *J* = 7.1 Hz, 3H), 1.24 (d, *J* = 6.0 Hz, 6H), 1.33–1.44 (m, 2H), 1.54–1.69 (m, 2H), 2.67 (t, *J* = 7.8 Hz, 2H), 3.58 (s, 2H), 4.40–4.60 (m, 1H), 7.29–7.33 (m, 2H), 7.47–7.53 (m, 3H), 7.71 (d, *J* = 3.6 Hz, 1H), 8.27 (br s, 1H), 10.30 (br s, 1H). ¹³C NMR [(CD₃)₂CO] δ: 14.16, 21.31, 22.93, 34.15, 36.14, 56.36, 80.22, 80.65, 98.04, 119.51, 129.67, 132.37, 132.68, 133.02, 136.41, 145.84. Anal. (C₂₁H₂₆N₂O₅S₂) C, H, N.

General Procedure for the Preparation of Esters 15h–l. A solution of aryl bromide **14** (800 mg, 1.93 mmol) in anhydrous dioxane (19.3 mL)/H₂O (4.2 mL) was sequentially treated under nitrogen with K₃PO₄ (942.5 mg, 4.44 mmol), the appropriate arylboronic acid (3.28 mmol), and Pd(PPh₃)₄ (223 mg, 0.19 mmol). The resulting mixture was stirred for 20 min at 70 °C. After being cooled to RT, the mixture was treated with NaHCO₃ and extracted with EtOAc. The combined organic extracts were dried over anhydrous Na₂SO₄, filtered, and evaporated under reduced pressure.

***tert*-Butyl 2-(5-(4-Fluorophenyl)-*N*-isopropoxythiophene-2-sulfonamido)acetate (15h).** The title compound was prepared from aryl bromide **14** and 4-fluorophenylboronic acid following the general procedure. The crude was purified by flash chromatography on silica gel (*n*-hexane/EtOAc 6:1) to give a pale-yellow oil (25% yield). ¹H NMR (CDCl₃) δ: 1.29 (d, *J* = 6.4 Hz, 6H), 1.47 (s, 9H), 3.68 (br s, 2H), 4.60 (septet, *J* = 6.2 Hz, 1H), 7.09–7.17 (m, 2H), 7.56–7.63 (m, 2H).

***tert*-Butyl 2-(5-(4-Ethylphenyl)-*N*-isopropoxythiophene-2-sulfonamido)acetate (15i).** The title compound was prepared from aryl bromide **14** and 4-ethylphenylboronic acid following the general procedure. The crude was purified by flash chromatography (*n*-hexane/EtOAc 30:1) using a ISOLUTE FLASH Si II cartridge (STEPBIO) to give **15i** as a yellow oil (26% yield). ¹H NMR (CDCl₃) δ: 1.22–1.30 (m, 8H), 1.47 (s, 9H), 2.68 (q, *J* = 7.6 Hz, 2H), 3.68 (br s, 2H), 4.59 (septet, *J* = 6.2 Hz, 1H), 7.23–7.29 (m, 3H), 7.51–7.55 (m, 2H), 7.61 (d, *J* = 3.8 Hz, 1H).

***tert*-Butyl 2-(*N*-isopropoxy-5-(4-methoxyphenyl)thiophene-2-sulfonamido)acetate (15l).** The title compound was prepared from aryl bromide **14** and 4-methoxyphenylboronic acid following the general procedure. The crude was purified by flash chromatography on silica gel (*n*-hexane/EtOAc 6:1) to give **15l** as a pale-yellow oil (54% yield). ¹H NMR (CDCl₃) δ: 1.29 (d, *J* =

6.2 Hz, 6H), 1.47 (s, 9H), 3.85 (s, 3H), 4.60 (septet, *J* = 6.2 Hz, 1H), 6.91–6.98 (m, 2H), 7.22 (d, *J* = 4.0 Hz, 1H), 7.51–7.57 (m, 2H), 7.60 (d, *J* = 4.0 Hz, 1H).

General Procedure for the Preparation of Carboxylic Acids 16h–l. TFA (0.8 mL, 10.26 mmol) was added dropwise to a stirred, ice-chilled solution of *tert*-butyl esters **15h–l** (0.18 mmol) in freshly distilled dichloromethane (1.4 mL). The mixture was stirred under these reaction conditions for 5 h, and the solvent was removed in vacuo to give the carboxylic acids **16h–l**. The crude products were purified by trituration with *n*-hexane/Et₂O.

2-(5-(4-Fluorophenyl)-*N*-isopropoxythiophene-2-sulfonamido)-acetic Acid (16h). The title compound was prepared from *tert*-butyl ester **15h** following the general procedure. Pale-yellow oil (90% yield). ¹H NMR (CDCl₃) δ: 1.28 (d, *J* = 6.4 Hz, 6H), 3.86 (br s, 2H), 4.60 (septet, *J* = 6.2 Hz, 1H), 5.87 (br s, 1H), 7.11 (d, *J* = 8.4 Hz, 1H), 7.16 (d, *J* = 8.6 Hz, 1H), 7.27 (d, *J* = 4.0 Hz, 1H), 7.56–7.60 (m, 2H), 7.64 (d, *J* = 4.0 Hz, 1H).

2-(5-(4-Ethylphenyl)-*N*-isopropoxythiophene-2-sulfonamido)-acetic Acid (16i). The title compound was prepared from *tert*-butyl ester **15i** following the general procedure. Pale-yellow solid (88% yield); mp 90–91 °C. ¹H NMR (CDCl₃) δ: 1.22–1.30 (m, 8H), 2.69 (q, *J* = 7.5 Hz, 2H), 3.87 (s, 2H), 4.60 (septet, *J* = 6.2 Hz, 1H), 7.25–7.31 (m, 3H), 7.52–7.56 (m, 2H), 7.64 (d, *J* = 3.8 Hz, 1H).

2-(*N*-isopropoxy-5-(4-methoxyphenyl)thiophene-2-sulfonamido)-acetic Acid (16l). The title compound was prepared from *tert*-butyl ester **15l** following the general procedure. Pale-yellow solid (90% yield); mp 135–137 °C. ¹H NMR (CDCl₃) δ: 1.29 (d, *J* = 6.2 Hz, 6H), 3.85 (s, 5H), 4.59 (septet, *J* = 6.2 Hz, 1H), 6.93–6.97 (m, 2H), 7.23 (d, *J* = 3.8 Hz, 1H), 7.52–7.57 (m, 2H), 7.62 (d, *J* = 3.8 Hz, 1H).

General Procedure to Synthesize Hydroxamic Acids 4h–l. 1-[3-(Dimethylamino)propyl]-3-ethyl carbodiimide hydrochloride (EDC) was added portionwise (72 mg, 0.37 mmol) to a stirred and cooled solution (0 °C) of the appropriate carboxylic acid **16h–l** (0.25 mmol) and *O*-(*tert*-butyldimethylsilyl)hydroxylamine (36.8 mg, 0.25 mmol) in freshly distilled CH₂Cl₂ (5.3 mL). After stirring at room temperature overnight, the mixture was washed with water and the organic phase was dried and evaporated in vacuo to afford the *O*-silylate intermediate. TFA (6.5 mL, 0.5 mmol) was added dropwise to a stirred and ice-chilled solution of the appropriate *O*-silylate (0.11 mmol) in CH₂Cl₂ (0.9 mL). The solution was stirred under these reaction conditions for 5 h, and the solvent was removed in vacuo. The crude products were purified by trituration with *n*-hexane/Et₂O to give the desired hydroxamates **4h–l**.

2-(5-(4-Fluorophenyl)-*N*-isopropoxythiophene-2-sulfonamido)-*N*-hydroxyacetamide (4h). The title compound was prepared from the carboxylic acid **16h** following the general procedure. White solid (89% yield); mp 75–76 °C. ¹H NMR (CDCl₃) δ: 1.27 (d, *J* = 6.0 Hz, 6H), 3.83 (s, 2H), 4.50 (septet, *J* = 6.4 Hz, 1H), 7.11 (d, *J* = 8.2 Hz, 1H), 7.16 (d, *J* = 8.2 Hz, 1H), 7.25–7.29 (m, 1H), 7.55–7.62 (m, 2H), 7.65 (d, *J* = 3.8 Hz, 1H). ¹³C NMR [(CD₃)₂CO] δ: 21.35, 56.36, 80.04, 117.12 (d, *J*_{C–F} = 21.9 Hz), 124.75, 129.30 (d, *J*_{C–F} = 8.2 Hz), 129.83, 137.48, 153.07, 161.68, 163.36, 166.62. Anal. (C₁₅H₁₇FN₂O₅S₂) C, H, N.

2-(5-(4-Ethylphenyl)-*N*-isopropoxythiophene-2-sulfonamido)-*N*-hydroxyacetamide (4i). The title compound was prepared from the carboxylic acid **16i** following the general procedure. White solid (89.6% yield); mp 113–114 °C. ¹H NMR (CDCl₃) δ: 1.22–1.29 (m, 8H), 2.69 (q, *J* = 7.5 Hz, 2H), 3.83 (s, 2H), 4.50 (septet, *J* = 5.6 Hz, 1H), 7.25–7.31 (m, 3H), 7.51–7.55 (m, 2H), 7.65 (d, *J* = 3.3 Hz, 1H). ¹³C NMR [(CD₃)₂CO] δ: 15.82, 21.35, 56.36, 79.96, 124.06, 127.07, 129.65, 130.38, 130.75, 137.46, 146.88, 154.60, 163.34. Anal. (C₁₇H₂₂N₂O₅S₂) C, H, N.

***N*-Hydroxy-2-(*N*-isopropoxy-5-(4-methoxyphenyl)thiophene-2-sulfonamido)acetamide (4l).** The title compound was prepared from the carboxylic acid **16l** following the general procedure. White solid (71% yield); mp 138–140 °C. ¹H NMR (CDCl₃)

δ : 1.27 (d, $J = 6.2$ Hz, 6H), 3.82 (s, 2H), 3.86 (s, 3H), 4.49 (septet, $J = 6.2$ Hz, 1H), 6.93–6.97 (m, 2H), 7.23 (d, $J = 4.0$ Hz, 1H), 7.52–7.56 (m, 2H), 7.63 (d, $J = 4.0$ Hz, 1H). ^{13}C NMR (CDCl_3) δ : 21.31, 55.62, 56.67, 80.32, 114.79, 122.37, 125.06, 127.54, 127.96, 137.08, 155.20, 160.88, 164.70. Anal. ($\text{C}_{16}\text{H}_{20}\text{N}_2\text{O}_6\text{S}_2$) C, H, N.

(*R*)-*tert*-Butyl 2-(4-Bromo-*N*-isopropoxyphenylsulfonamido)-3-methylbutanoate (**18**). Diisopropyl azodicarboxylate (DIAD) (2.5 mL, 12.5 mmol) was added dropwise to a solution containing (*S*)-*tert*-butyl 2-hydroxy-3-methylbutanoate **17** (0.87 g, 5.0 mmol), the sulfonamide **6** (2.2 g, 7.5 mmol), and triphenylphosphine (3.9 g, 15 mmol) in anhydrous THF (60 mL) under nitrogen atmosphere at 0 °C. The resulting solution was stirred for 5 h at RT and evaporated under reduced pressure to afford a crude product, which was purified by flash chromatography on silica gel (*n*-hexane/EtOAc = 40:1) to yield **18** (1.9 g, 84%) as pure-yellow oil. ^1H NMR (CDCl_3) δ : 0.88 (d, $J = 6.4$ Hz, 3H), 1.15 (br s, 9H), 1.25 (t, $J = 6.7$ Hz, 9H), 2.10–2.36 (m, 1H), 3.67 (d, $J = 10.6$ Hz, 1H), 4.42 (septet, $J = 6.2$ Hz, 1H), 7.63–7.68 (m, 2H), 7.75–7.80 (m, 2H).

(*R*)-*tert*-Butyl 2-(4-(4-Chlorobenzoyloxy)-*N*-isopropoxybiphenyl-4-ylsulfonamido)-3-methylbutanoate (**19**). A mixture of aryl bromide **18** (300 mg, 0.66 mmol), 4-(4'-chlorobenzoyloxy)phenylboronic acid (295 mg, 1.12 mmol), Pd(PPh_3)₄ (38 mg, 0.03 mmol), and K_3PO_4 (322 mg, 1.5 mmol) in dioxane (6.6 mL)/ H_2O (1.5 mL) was heated at 70 °C under nitrogen. After 1 h, the reaction mixture was diluted with sat. solution of NaHCO_3 , extracted with EtOAc, and dried over Na_2SO_4 . The organic layer was concentrated in vacuo, and the crude product was purified by flash chromatography (*n*-hexane/EtOAc = 20:1) using a ISOLUTE FLASH Si II cartridge (STEPBIO) to give **19** as a white solid (230 mg, 67% yield). ^1H NMR (CDCl_3) δ : 0.89 (d, $J = 6.6$ Hz, 3H), 1.10 (br s, 9H), 1.27 (t, $J = 6.4$ Hz, 9H), 2.12–2.40 (m, 1H), 3.75 (d, $J = 10.6$ Hz, 1H), 4.45 (septet, $J = 6.4$ Hz, 1H), 5.09 (s, 2H), 7.03–7.07 (m, 2H), 7.38 (s, 4H), 7.51–7.56 (m, 2H), 7.64–7.69 (m, 2H), 7.93–7.97 (m, 2H).

(*R*)-2-(4'-(4-Chlorobenzoyloxy)-*N*-isopropoxybiphenyl-4-ylsulfonamido)-3-methylbutanoic Acid (**20**). TFA (1.75 mL, 22.8 mmol) was added dropwise to a stirred, ice-chilled solution of *tert*-butyl ester **19** (230 mg, 0.4 mmol) in freshly distilled dichloromethane (4 mL). The mixture was stirred under these reaction conditions for 5 h, and the solvent was removed in vacuo. The crude product was purified by trituration with *n*-hexane/ Et_2O to give the carboxylic acid **20** (167 mg, 78% yield) as a white solid; mp 92–93 °C; $[\alpha]_D^{20} + 83^\circ$ (c 0.07, CHCl_3). ^1H NMR (CDCl_3) δ : 0.91 (d, $J = 6.6$ Hz, 3H), 1.02–1.22 (m, 3H), 1.24 (d, $J = 6.2$ Hz, 3H), 1.30 (d, $J = 6.2$ Hz, 3H), 2.08–2.22 (m, 1H), 3.90 (d, $J = 10.2$ Hz, 1H), 4.48 (septet, $J = 6.2$ Hz, 1H), 5.09 (s, 2H), 7.03–7.07 (m, 2H), 7.38 (s, 4H), 7.54–7.58 (m, 2H), 7.63–7.67 (m, 2H), 7.88–7.92 (m, 2H).

(*R*)-2-(4'-(4-Chlorobenzoyloxy)-*N*-isopropoxybiphenyl-4-ylsulfonamido)-*N*-hydroxy-3-methylbutanamide (**5**). 1-[3-(Dimethylamino)propyl]-3-ethyl carbodiimide hydrochloride (EDC) was added portionwise (86.2 mg, 0.4 mmol) to a stirred and cooled solution (0 °C) of the carboxylic acid **20** (160 mg, 0.3 mmol) and *O*-(*tert*-butyldimethylsilyl)hydroxylamine (44.2 mg, 0.3 mmol) in freshly distilled CH_2Cl_2 (7 mL). After stirring at room temperature overnight, the mixture was washed with water and the organic phase was dried and evaporated in vacuo. The crude was purified by flash chromatography (*n*-hexane/EtOAc 6:1) using a ISOLUTE FLASH Si II cartridge (STEPBIO) to afford the *O*-silylate intermediate (121 mg, 61% yield) as a yellow oil. ^1H NMR (CDCl_3) δ : 0.06 (s, 6H), 0.84–0.93 (m, 12H), 1.22–1.26 (m, 9H), 2.05–2.27 (m, 1H), 4.33–4.40 (m, 1H), 5.09 (s, 2H), 7.02–7.06 (m, 2H), 7.38 (s, 4H), 7.55–7.59 (m, 2H), 7.69–7.73 (m, 2H), 7.90–7.95 (m, 2H).

TFA (0.8 mL, 10.26 mmol) was added dropwise to a stirred and ice-chilled solution of *O*-silylate (120 mg, 0.18 mmol) in CH_2Cl_2 (2 mL). The solution was stirred under these reaction conditions for 5 h, and the solvent was removed in vacuo. The crude product was purified by trituration with *n*-hexane/ Et_2O to

give the hydroxamate **5** as a white solid (78 mg, 80% yield); mp 94–95 °C; $[\alpha]_D^{20} + 65^\circ$ (c 0.1, CHCl_3). ^1H NMR (CDCl_3) δ : 0.92 (d, $J = 6.4$ Hz, 3H), 0.96–1.22 (m, 3H), 1.30 (d, $J = 6.4$ Hz, 3H), 1.36 (d, $J = 6.2$ Hz, 3H), 1.92–2.12 (m, 1H), 3.92 (br s, 1H), 4.53 (septet, $J = 6.4$ Hz, 1H), 5.09 (s, 2H), 7.02–7.06 (m, 2H), 7.37 (s, 4H), 7.53–7.57 (m, 2H), 7.67–7.71 (m, 2H), 7.87–7.91 (m, 2H). ^{13}C NMR (CDCl_3) δ : 19.47, 20.76, 21.66, 69.47, 70.25, 81.58, 115.54, 126.97, 128.72, 128.85, 128.94, 130.07, 131.89, 132.05, 134.02, 135.22, 146.67, 159.24. Anal. ($\text{C}_{27}\text{H}_{31}\text{ClN}_2\text{O}_6\text{S}$) C, H, N.

MMP Inhibition Assays.⁴⁹ Recombinant human MMP-14 and MMP-16 catalytic domains were a kind gift of Prof. Gillian Murphy (Department of Oncology, University of Cambridge, UK). pro-MMP-1, pro-MMP-2, pro-MMP-3, pro-MMP-8, pro-MMP-9, pro-MMP-13, and TACE (ADAM-17) were purchased from Calbiochem.

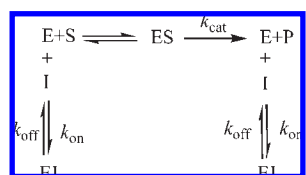
Proenzymes were activated immediately prior to use with *p*-aminophenylmercuric acetate (APMA 2 mM for 1 h at 37 °C for MMP-2, MMP-1, and MMP-8, 1 mM for 1 h at 37 °C for MMP-9 and MMP-13). Pro-MMP-3 was activated with trypsin 5 $\mu\text{g}/\text{mL}$ for 30 min at 37 °C, followed by soybean trypsin inhibitor 62 $\mu\text{g}/\text{mL}$. For assay measurements, the inhibitor stock solutions (100 mM in DMSO) were further diluted, at seven different concentrations (0.01 nM–300 μM) for each MMP in the fluorimetric assay buffer (FAB: Tris 50 mM, pH = 7.5, NaCl 150 mM, CaCl_2 10 mM, Brij 35 0.05%, and DMSO 1%). Activated enzyme (final concentration 2.9 nM for MMP-2, 2.7 nM for MMP-9, 1.5 nM for MMP-8, 0.3 nM for MMP-13, 5 nM for MMP-3, 1 nM for MMP-14 cd, 15 nM for MMP-16 cd, 2.0 nM for MMP-1, and 7.5 nM for TACE) and inhibitor solutions were incubated in the assay buffer for 4 h at 25 °C. TACE was incubated for 20 min at 25 °C. After the addition of 200 μM solution of the fluorogenic substrate Mca-Arg-Pro-Lys-Pro-Val-Glu-Nva-Trp-Arg-Lys-(Dnp)- NH_2 (Sigma) for MMP-3 and Mca-Lys-Pro-Leu-Gly-Leu-Dap(Dnp)-Ala-Arg- NH_2 (Bachem) for all the other enzymes in DMSO (final concentration 2 μM), the hydrolysis was monitored every 15 s for 15 min recording the increase in fluorescence ($\lambda_{\text{ex}} = 325$ nm, $\lambda_{\text{em}} = 395$ nm) using a Molecular Devices SpectraMax Gemini XS plate reader. The assays were performed in triplicate in a total volume of 200 μL per well in 96-well microtiter plates (Corning, black, NBS). The MMP inhibition activity was expressed in relative fluorescent units (RFU). Percent of inhibition was calculated from control reactions without the inhibitor. IC_{50} was determined using the formula: $V_i/V_o = 1/(1 + [I]/\text{IC}_{50})$, where V_i is the initial velocity of substrate cleavage in the presence of the inhibitor at concentration $[I]$ and V_o is the initial velocity in the absence of the inhibitor. Results were analyzed using SoftMax Pro software⁵⁰ and GraFit software.⁵¹

Slow-Binding Inhibition Assay. For slow-binding inhibition measurements, the inhibitor stock solutions (10 mM in DMSO) were further diluted at four different concentrations (50–480 nM for **5**, 10–80 nM for **4d**, 2–40 nM for **4b**, 5–150 nM for **1a**, and 2–20 nM for **1b**). After the addition of the enzyme (the final concentration was 1.3 nM for MMP-13 and 1.4 nM for MMP-2) to the solution containing substrate and inhibitor, the hydrolysis of the fluorogenic substrate was monitored every 3 s for 15 min at 25 °C as described above. The control reactions do not contain inhibitor. Data were fitted to the following equation⁵² by SigmaPlot 9.0 Software: $\Delta F = \nu_f t + [(v_0 - \nu_f)1 - e^{-k_{\text{obs}}t}]/k_{\text{obs}}$ where ΔF is the variation of fluorescence, ν_f is the steady state velocity, v_0 is the initial velocity, and k_{obs} is the apparent first-order rate constant for slow-binding. Association and dissociation rate constants (k_{on} and k_{off} , respectively) were obtained from the slope and intercept, respectively, of plots of the k_{obs} values versus the inhibitor concentration according to the equation:⁵² $k_{\text{obs}} = k_{\text{off}} + k_{\text{on}}[I]/(1 + [S]/K_M)$.

This equation describes a one-step association mechanism (Scheme 4) where *S* is the fluorogenic substrate used and EI is the complex between the enzyme and the inhibitor. Under our

conditions, the concentration of substrate is well below K_M , thus the term $[S]/K_M$ could be neglected. The $k_{\text{off}}/k_{\text{on}}$ ratio gives the K_i value.

Scheme 4



Collagenase Assays. MMP-1 (0.5 nM) or MMP-13 (1 nM) was preincubated with the different inhibitors at a range of concentrations (0–10 μM) for 2 h at 25 °C in collagenase buffer (50 mM Tris HCl pH 7.5, 150 mM NaCl, 5 mM CaCl₂, 0.05% Brij-35, 0.02% NaN₃). Acid soluble collagen purified from guinea pig skin neutralized with collagenase buffer was added to bring the final concentration of substrate to 1.35 mg/mL. The reactions were incubated for a further 16 h at 25 °C, before the reactions were stopped with SDS-PAGE loading buffer containing 50 mM EDTA. The amount of collagen degradation was determined by densitometric quantification of the full length and 3/4 cleaved fragment of the α 2-chain of collagen following SDS-PAGE separation (7.5% acrylamide) and staining with Coomassie Brilliant Blue-R250 using the Biorad GS-710 calibrated scanning densitometer and analyzed using the Phoretix 1D software (Nonlinear Dynamics, Newcastle Upon Tyne, UK). The percentage of collagen cleavage was calculated according to the method of Welgus et al.⁵²

Cartilage Degradation Assays. Porcine articular cartilage from the metacarpophalangeal joints of 3–9 month old pigs were dissected and cut into pieces approximately 0.5 mm \times 3 mm \times 3 mm. After dissection, cartilage explants were allowed to rest for 24 h at 37 °C under 5% CO₂ in DMEM containing 100 U/mL penicillin, 100 mg/mL streptomycin, 10 mM HEPES, and 10% fetal calf serum (FCS) before switching to media without FCS for a further 3 days. Rested explants were stimulated with 10 ng/mL IL-1 α with the inhibitors at 0.1, 1, and 10 μM , respectively, in serum free medium. The medium was changed every 3–4 days for the duration of the experiment. Glycosaminoglycan (GAG) and hydroxyproline (Hypro) released into the medium was taken as measures of aggrecan and collagen degradation, respectively. The amount of GAG released was standardized against shark/whale chondroitin sulfate (Sigma) using the dimethylmethylene blue (DMMB) assay modified for use in a 96-well plate.³⁴ Hypro released into the culture media was determined using a modification of the assay as described by Bergman and Loxley.⁵³ Briefly, conditioned media (50 μL) was acid hydrolyzed by the addition of an equal volume of 6 N HCl for 20 h at 95 °C in a microcentrifuge tube. The acid was removed from the hydrolyzed residue by drying in a vacuum centrifuge for 4 h. The dried residue was fully resuspended in 40 μL dH₂O. The sample was reacted with 25 μL chloramine T reagent (1.4% (w/v) chloramine T, 30.8% (v/v) isopropanol, 335 mM NaOAc, 100 mM trisodium citrate, 23 mM citric acid) for 4 min at room temperature before addition of 150 μL of dimethylaminobenzaldehyde (DMBA) reagent (16.7% (w/v) DMBA, 75% (v/v) isopropanol, 52.5% (v/v) perchloric acid). The mixture was incubated at 70 °C for 40 min and left to cool before the absorbance at 560 nm was read. The amount of hydroxyproline was calculated by comparison to a standard curve (0–1.2 μg L-hydroxyproline).

Molecular Modeling. Docking Simulations. Molecular docking of compound **5** into the three-dimensional X-ray structure of the metalloenzymes was carried out using the AutoDock software package (version 4.0) as implemented through the graphical user interface AutoDockTools (ADT 1.5.1).⁵⁴

Ligands and Protein Setup. The inhibitor structure was first generated through the Dundee PRODRG2 Server.⁵⁵ Then the

Cambridge Structural Database was searched to find the preferred torsion values for the *N*-isopropoxy aryl sulfonamide. As no one example for acyclic *N*-isopropoxy aryl sulfonamide was found, we approached the problem in two steps by assessing first the Car-Car-S-N torsion of the aryl sulfonamides devoid of any ortho substituents, and a clear preference for a 90° dihedral angle has been found regardless the substituents on the nitrogen atom. On the basis of these findings, we simplified the query excluding the aryl moiety founding 14 acyclic N-O sulfonamides. Now, plotting the torsion O-S-N-X or O-S-N-O (data not shown), it resulted that independently from the substituents on the N, two preferred conformations have been found. The most populated one is that in which the N-lone pair bisects the O=S=O angle, while the other one occurs when one N-substituent bisects the O=S=O angle.

Because Autodock force fields have no parameters describing the lowest energy conformations of groups of atoms and in the case of *N*-bisubstituted arylsulfonamides, it distorted the low-energy conformations, giving rise to conformations which are unlikely to exist, we decided to keep the torsions involving the Car-S and S-N bond fixed using the values found as preferred in the CSD. Thus, the ligand in the two possible conformers was docked, considering also the symmetric geometries and the N-pyramidal inversion.

The hydroxamate moiety was considered in its singly deprotonated form (hydroxamate), in line with previous experimental studies.⁵⁶

The parametrization of **5** for the docking experiments was performed using the Gaussian03 package⁵⁷ by applying a full geometry optimization at Hartree-Fock level of theory and calculating the charges using the restrained electrostatic potential (RESP) fitting procedure.^{58,59} For both the optimization and the electrostatic potential calculation, the locally dense 6-31G* basis set was used.

With regard to the protein setup, to create initial coordinates for docking studies, calcium ions, cocrystallized inhibitors, and all water molecules of the crystal structures were removed and excluded from calculations. For the zinc atom, an ion parametrization, specific for the hydroxamic chelators and based on quantum chemistry calculations, was used as suggested by Cheng et al.⁶⁰

Docking Setup. The docking area has been defined by a box, centered on the catalytic zinc atom. Grids points of 65 \times 60 \times 60 with 0.375 Å spacing were calculated around the docking area for all the ligand atom types using AutoGrid4. For inhibitor **5**, 100 separate docking calculations were performed. Each docking calculation consisted of 25 \times 10⁶ energy evaluations using the Lamarckian genetic algorithm local search (GALS) method. A low-frequency local search according to the method of Solis and Wets was applied to docking trials to ensure that the final solution represents a local minimum. Each docking run was performed with a population size of 150, and 300 rounds of Solis and Wets local search were applied with a probability of 0.06. A mutation rate of 0.02 and a crossover rate of 0.8 were used to generate new docking trials for subsequent generations. The docking results from each of the 100 calculations were clustered on the basis of root-mean-square deviation (rmsd = 2.0 Å) between the Cartesian coordinates of the ligand atoms and were ranked on the basis of the free energy of binding.

Energy Minimization of the Docked Complex. The lowest energy binding pose of **5** with MMP-13, as resulted from docking calculations, was subjected to an energy minimization by means of the AMBER 9.0 package software.⁶¹ Ligand force-field parameters were derived using the Antechamber program, and partial charges were calculated using the RESP methodology as described above. For the purpose of the energy minimization, the complex was first inserted in a box (68.524 Å \times 65.510 Å \times 71.425 Å) of TIP3P⁶² pre-equilibrated water molecules. Then, four Na⁺ ions were randomly placed by means of the add ions routine of Xleap to maintain neutrality in the

system. First, water molecules and counterions were minimized using steepest descent followed by conjugated gradient. Second, a minimization of the entire system was performed by means of 2000 steps of steepest descent followed by 3000 steps of conjugated gradient. The energy optimization was run for water solution using the particle mesh Ewald (PME) method⁶³ for the treatment of the long-range electrostatics; a 8.0 Å distance cutoff was used for direct space nonbonded calculations and a 0.00001 Ewald convergence tolerance for the inclusion of long-range electrostatic contributions; the SHAKE option (tolerance 0.00005 Å) was used for constraining bonds involving hydrogen atoms. Visual inspection of docking results were made with MGL-Tools package,⁶⁴ and Figure 5 was rendered by the Chimera software package.⁶⁵

Acknowledgment. We are grateful for financial support given by MIUR (Prin 2007) and by the Fondazione Monte dei Paschi di Siena (“Strumenti terapeutici innovative per la modulazione dell’attività di metalloproteasi della matrice implicate nelle patologie tumorali cerebrali”).

Supporting Information Available: A table reporting the HPLC purity analysis and the combustion analysis data of the final products. This material is available free of charge via the Internet at <http://pubs.acs.org>.

References

- Inada, M.; Wang, Y.; Byrne, M. H.; Rahman, M. U.; Miyaura, C.; López-Otín, C.; Krane, S. M. Critical roles for collagenase-3 (Mmp13) in development of growth plate cartilage and in endochondral ossification. *Proc. Natl. Acad. Sci. U.S.A.* **2004**, *101*, 17192–17197.
- Ishikawa, T.; Nishigaki, F.; Miyata, S.; Hirayama, Y.; Minoura, K.; Imanishi, J.; Neya, M.; Mizutani, T.; Imamura, Y.; Ohkubo, Y.; Mutoh, S. Prevention of progressive joint destruction in adjuvant induced arthritis in rats by a novel matrix metalloproteinase inhibitor, FR217840. *Eur. J. Pharmacol.* **2005**, *508*, 239–247.
- Murphy, G.; Nagase, H. Reappraising metalloproteinases in rheumatoid arthritis and osteoarthritis: destruction or repair? *Nat. Clin. Pract. Rheumatol.* **2008**, *4*, 128–135.
- Fingleton, B. Matrix metalloproteinases as valid clinical targets. *Curr. Pharm. Des.* **2007**, *13*, 333–346.
- Johnson, A. R.; Pavlovsky, A. G.; Ortwine, D. F.; Prior, F.; Man, C. F.; Bornemeier, D. A.; Banotai, C. A.; Mueller, W. T.; McConnell, P.; Yan, C.; Baragi, V.; Lesch, C.; Roark, W. H.; Wilson, M.; Datta, K.; Guzman, R.; Han, H. K.; Dyer, R. D. Discovery and characterization of a novel inhibitor of matrix metalloprotease-13 that reduces cartilage damage in vivo without joint fibroplasia side effects. *J. Biol. Chem.* **2007**, *282*, 27781–27791.
- Billinghurst, R. C.; Dahlberg, L.; Ionescu, M.; Reiner, A.; Bourne, R.; Rorabeck, C.; Mitchell, P.; Hambor, J.; Diekmann, O.; Tschesche, H.; Chen, J.; Van Wart, H.; Poole, A. R. Enhanced cleavage of type II collagen by collagenases in osteoarthritic articular cartilage. *J. Clin. Invest.* **1997**, *99*, 1534–1545.
- Coussens, L. M.; Fingleton, B.; Matrisian, L. M. Matrix metalloproteinase inhibitors and cancer: trials and tribulations. *Science* **2002**, *295*, 2387–2392.
- Naglich, J. G.; Jure-Kunkel, M.; Gupta, E.; Fargnoli, J.; Henderson, A. J.; Lewin, A. C.; Talbott, R.; Baxter, A.; Bird, J.; Savopoulos, R.; Wills, R.; Kramer, R. A.; Trail, P. A. Inhibition of angiogenesis and metastasis in two murine models by the matrix metalloproteinase inhibitor, BMS-275291. *Cancer Res.* **2001**, *61*, 8480–8485.
- Wu, J.; Rush, T. S.III; Hotchandani, R.; Du, X.; Geck, M.; Collins, E.; Xu, Z. B.; Skotnicki, J.; Levin, J. I.; Lovering, F. E. Identification of potent and selective MMP-13 inhibitors. *Bioorg. Med. Chem. Lett.* **2005**, *15*, 4105–4109.
- Li, J.; Rush, T. S.III; Li, W.; DeVincentis, D.; Du, X.; Hu, Y.; Thomason, J. R.; Xiang, J. S.; Skotnicki, J. S.; Tam, S.; Cunningham, K. M.; Chockalingam, P. S.; Morris, E. A.; Levin, J. I. Synthesis and SAR of highly selective MMP-13 inhibitors. *Bioorg. Med. Chem. Lett.* **2005**, *15*, 4961–4966.
- Hu, Y.; Xiang, J. S.; DiGrandi, M. J.; Du, X.; Ipek, M.; Laakso, L. M.; Li, J.; Li, W.; Rush, T. S.; Schmid, J.; Skotnicki, J. S.; Tam, S.; Thomason, J. R.; Wang, Q.; Levin, J. I. Potent, selective, and orally bioavailable matrix metalloproteinase-13 inhibitors for the treatment of osteoarthritis. *Bioorg. Med. Chem.* **2005**, *13*, 6629–6644.
- Aranapakam, V.; Davis, J. M.; Grosu, G. T.; Baker, J.; Ellingboe, J.; Zask, A.; Levin, J. I.; Sandanayaka, V. P.; Du, M.; Skotnicki, J. S.; Di Joseph, J. F.; Sung, A.; Sharr, M. A.; Killar, L. M.; Walter, T.; Jin, G.; Cowling, R.; Tillett, J.; Zhao, W.; McDevitt, J.; Xu, Z. B. Synthesis and structure–activity relationship of *N*-substituted 4-arylsulfonylpiperidine-4-hydroxamic acids as novel, orally active matrix metalloproteinase inhibitors for the treatment of osteoarthritis. *J. Med. Chem.* **2003**, *46*, 2376–2396.
- Augé, F.; Hornebeck, W.; Decarme, M.; Laronze, J. Y. Improved gelatinase a selectivity by novel zinc binding groups containing galardin derivatives. *Bioorg. Med. Chem. Lett.* **2003**, *13*, 1783–1786.
- Rush, T. S.III; Powers, R. The Application of X-ray, NMR, and Molecular Modeling in the Design of MMP Inhibitors. *Curr. Top. Med. Chem.* **2004**, *4*, 1311–1327.
- Chen, J. M.; Nelson, F. C.; Levin, J. I.; Mobilio, D.; Moy, F. J.; Nilakantan, R.; Zask, A.; Powers, R. Structure-Based Design of a Novel, Potent, and Selective Inhibitor for MMP-13 Utilizing NMR Spectroscopy and Computer-Aided Molecular Design. *J. Am. Chem. Soc.* **2000**, *122*, 9648–9654.
- (a) Engel, C. K.; Pirard, B.; Schimanski, S.; Kirsch, R.; Habermann, J.; Klingler, O.; Schlotte, V.; Weithmann, K. U.; Wendt, K. U. Structural basis for the highly selective inhibition of MMP-13. *Chem. Biol.* **2005**, *12*, 181–189. (b) Li, J. J.; Nagra, J.; Johnson, A. R.; Bunker, A.; O'Brien, P.; Yue, W. S.; Ortwine, D. F.; Man, C. F.; Baragi, V.; Kilgore, K.; Dyer, R. D.; Han, H. K. Quinazolinones and pyrido-[3,4-d]pyrimidin-4-ones as orally active and specific matrix metalloproteinase-13 inhibitors for the treatment of osteoarthritis. *J. Med. Chem.* **2008**, *51*, 835–841.
- Rossello, A.; Nuti, E.; Orlandini, E.; Carelli, P.; Rapposelli, S.; Macchia, M.; Minutolo, F.; Carbonaro, L.; Albini, A.; Benelli, R.; Cercignani, G.; Murphy, G.; Balsamo, A. New *N*-arylsulfonyl-*N*-alkoxyaminoacetohydroxamic acids as selective inhibitors of gelatinase A (MMP-2). *Bioorg. Med. Chem.* **2004**, *12*, 2441–2450.
- Cheng, X. C.; Wang, Q.; Fang, H.; Xu, W. F. Role of sulfonamide group in matrix metalloproteinase inhibitors. *Curr. Med. Chem.* **2008**, *15*, 368–373.
- Marques, S. M.; Nuti, E.; Rossello, A.; Supuran, C. T.; Tuccinardi, T.; Martinelli, A.; Santos, M. A. Dual Inhibitors of Matrix Metalloproteinases and Carbonic Anhydrases: Iminodiacetyl-Based Hydroxamate-Benzenesulfonamide Conjugates. *J. Med. Chem.* **2008**, *51*, 7968–7979.
- Lovejoy, B.; Welch, A.; Carr, S.; Luong, C.; Broka, C.; Hendricks, R. T.; Campbell, J.; Walker, K.; Martin, R.; Van Wart, H.; Browner, M. F. Crystal structures of MMP-1 and -13 reveal the structural basis for selectivity of collagenase inhibitors. *Nat. Struct. Biol.* **1999**, *6*, 217–221.
- Moy, F. J.; Chanda, P. K.; Chen, J. M.; Cosmi, S.; Edris, W.; Levin, J. I.; Powers, R. High-resolution solution structure of the catalytic fragment of human collagenase-3 (MMP-13) complexed with a hydroxamic acid inhibitor. *J. Mol. Biol.* **2000**, *302*, 671–689.
- Zhang, X.; Gonnella, N. C.; Koehn, J.; Pathak, N.; Ganu, V.; Melton, R.; Parker, D.; Hu, S. I.; Nam, K. Y. Solution structure of the catalytic domain of human collagenase-3 (MMP-13) complexed to a potent non-peptidic sulfonamide inhibitor: binding comparison with stromelysin-1 and collagenase-1. *J. Mol. Biol.* **2000**, *301*, 513–524.
- Kohno, T.; Hochigai, H.; Yamashita, E.; Tsukihara, T.; Kanaoka, M. Crystal structures of the catalytic domain of human stromelysin-1 (MMP-3) and collagenase-3 (MMP-13) with a hydroxamic acid inhibitor SM-25453. *Biochem. Biophys. Res. Commun.* **2006**, *344*, 315–322.
- Bertini, I.; Calderone, V.; Fragai, M.; Giachetti, A.; Loconte, M.; Luchinat, C.; Maletta, M.; Nativi, C.; Yeo, K. J. Exploring the subtleties of drug–receptor interactions: the case of matrix metalloproteinases. *J. Am. Chem. Soc.* **2007**, *129*, 2466–2475.
- Rossello, A.; Nuti, E.; Orlandini, E.; Balsamo, A.; Tuccinardi, T. Compounds having aryl-sulphonamidic structure useful as metalloproteinase inhibitors. Patent WO2008113756, 2008.
- Nuti, E.; Orlandini, E.; Nencetti, S.; Rossello, A.; Innocenti, A.; Scozzafava, A.; Supuran, C. T. Carbonic anhydrase and matrix metalloproteinase inhibitors. Inhibition of human tumor-associated isozymes IX and cytosolic isozyme I and II with sulfonlated hydroxamates. *Bioorg. Med. Chem.* **2007**, *15*, 2298–2311.
- Sonogashira, K.; Tohda, Y.; Hagihara, N. A Convenient Synthesis of Acetylenes: Catalytic Substitutions of Acetylenic Hydrogen with Bromoalkenes, Iodoarenes, and Bromopyridines. *Tetrahedron Lett.* **1975**, *50*, 4467–4470.

- (28) Tuccinardi, T.; Martinelli, A.; Nutti, E.; Carelli, P.; Balzano, F.; Uccello-Barretta, G.; Murphy, G.; Rossello, A. Amber force field implementation, molecular modelling study, synthesis and MMP-1/MMP-2 inhibition profile of (*R*)- and (*S*)-*N*-hydroxy-2-(*N*-isopropoxybiphenyl-4-ylsulfonamido)-3-methylbutanamide. *Bioorg. Med. Chem.* **2006**, *14*, 4260–4276.
- (29) Neumann, U.; Kubota, H.; Frei, K.; Ganu, V.; Leppert, D. Characterization of Mca-Lys-Pro-Leu-Gly-Leu-Dpa-Ala-Arg-NH₂, a fluorogenic substrate with increased specificity constants for collagenases and tumor necrosis factor converting enzyme. *Anal. Biochem.* **2004**, *328*, 166–173.
- (30) Rossello, A.; Nutti, E.; Carelli, P.; Orlandini, E.; Macchia, M.; Nencetti, S.; Zandomeneghi, M.; Balzano, F.; Uccello-Barretta, G.; Albini, A.; Benelli, R.; Cercignani, G.; Murphy, G.; Balsamo, A. *N*-*i*-Propoxy-*N*-biphenylsulfonaminobutylhydroxamic acids as potent and selective inhibitors of MMP-2 and MT1-MMP. *Bioorg. Med. Chem. Lett.* **2005**, *15*, 1321–1326.
- (31) Ikejiri, M.; Bernardo, M. M.; Bonfil, R. D.; Toth, M.; Chang, M.; Fridman, R.; Mobashery, S. Potent mechanism-based inhibitors for matrix metalloproteinases. *J. Biol. Chem.* **2005**, *280*, 33992–34002.
- (32) Duggleby, R. G.; Attwood, P. V.; Wallace, J. C.; Keech, D. B. Avidin is a slow binding inhibitor of pyruvate carboxylase. *Biochemistry* **1982**, *21*, 3364–3370.
- (33) Cawston, T.; Plumptre, T.; Curry, V.; Ellis, A.; Powell, L. Role of TIMP and MMP inhibition in preventing connective tissue breakdown. *Ann. N.Y. Acad. Sci.* **1994**, *732*, 75–83.
- (34) Gendron, C.; Kashiwagi, M.; Hughes, C.; Caterson, B.; Nagase, H. TIMP-3 inhibits aggrecanase-mediated glycosaminoglycan release from cartilage explants stimulated by catabolic factors. *FEBS Lett.* **2003**, *555*, 431–436.
- (35) Jozic, D.; Bourenkov, G.; Lim, N. H.; Visse, R.; Nagase, H.; Bode, W.; Maskos, K. X-ray structure of human proMMP-1: new insights into procollagenase activation and collagen binding. *J. Biol. Chem.* **2005**, *280*, 9578–9585.
- (36) Iyer, S.; Visse, R.; Nagase, H.; Acharya, K. R. Crystal structure of an active form of human MMP-1. *J. Mol. Biol.* **2006**, *362*, 78–88.
- (37) Iyer, S.; Wei, S.; Brew, K.; Acharya, K. R. Crystal structure of the catalytic domain of matrix metalloproteinase-1 in complex with the inhibitory domain of tissue inhibitor of metalloproteinase-1. *J. Biol. Chem.* **2007**, *282*, 364–371.
- (38) Spurlino, J. C.; Smallwood, A. M.; Carlton, D. D.; Banks, T. M.; Vavra, K. J.; Johnson, J. S.; Cook, E. R.; Falvo, J.; Wahl, R. C.; Pulvino, T. A.; Wendoloski, J. J.; Smith, D. L. 1.56 Å Structure of mature truncated human fibroblast collagenase. *Proteins* **1994**, *19*, 98–109.
- (39) Borkakoti, N.; Winkler, F. K.; Williams, D. H.; D'Arcy, A.; Broadhurst, M. J.; Brown, P. A.; Johnson, W. H.; Murray, E. J. Structure of the catalytic domain of human fibroblast collagenase complexed with an inhibitor. *Nat. Struct. Biol.* **1994**, *1*, 106–110.
- (40) Bender, S. L.; Broka, C. A.; Campbell, J. A.; Castelano, A. L.; Fisher, L. E.; Hendricks, R. T.; Sarma, K. Preparation of arylthioalkanoates and analogs as matrix metalloprotease inhibitors. Patent EP 780386 A1 19970625, 1997.
- (41) Mazzola, R. D., Jr.; Zhu, Z.; Sinning, L.; McKittrick, B.; Lavey, B.; Spither, J.; Kozlowski, J.; Neng-Yang, S.; Zhou, G.; Guo, Z.; Orth, P.; Madison, V.; Sun, J.; Lundell, D.; Niu, X. Discovery of novel hydroxamates as highly potent tumor necrosis factor- α converting enzyme inhibitors. Part II: Optimization of the S3' pocket. *Bioorg. Med. Chem. Lett.* **2008**, *18*, 5809–5814.
- (42) Condon, J. S.; Joseph-McCarthy, D.; Levin, J. I.; Lombart, H. G.; Lovering, F. E.; Sun, L.; Wang, W.; Xu, W.; Zhang, Y. Identification of potent and selective TACE inhibitors via the S1 pocket. *Bioorg. Med. Chem. Lett.* **2007**, *17*, 34–39.
- (43) Govinda Rao, B.; Bandarage, U. K.; Wang, T.; Come, J. H.; Perola, E.; Wei, Y.; Tian, S. K.; Saunders, J. O. Novel thiol-based TACE inhibitors: rational design, synthesis, and SAR of thiol-containing aryl sulfonamides. *Bioorg. Med. Chem. Lett.* **2007**, *17*, 2250–2253.
- (44) Fernandez-Catalan, C.; Bode, W.; Huber, R.; Turk, D.; Calvete, J. J.; Lichte, A.; Tschesche, H.; Maskos, K. Crystal structure of the complex formed by the membrane type 1-matrix metalloproteinase with the tissue inhibitor of metalloproteinases-2, the soluble progelatinase A receptor. *EMBO J.* **1998**, *17*, 5238–48.
- (45) Maskos, K.; Fernandez-Catalan, C.; Huber, R.; Bourenkov, G. P.; Bartunik, H.; Ellestad, G. A.; Reddy, P.; Wolfson, M. F.; Rauch, C. T.; Castner, B. J.; Davis, R.; Clarke, H. R.; Petersen, M.; Fitzner, J. N.; Cerretti, D. P.; March, C. J.; Paxton, R. J.; Black, R. A.; Bode, W. Crystal structure of the catalytic domain of human tumor necrosis factor- α -converting enzyme. *Proc. Natl. Acad. Sci. U.S.A.* **1998**, *95*, 3408–3412.
- (46) Solomon, A.; Rosenblum, G.; Gonzales, P. E.; Leonard, J. D.; Mobashery, S.; Milla, M. E.; Sagi, I. Pronounced diversity in electronic and chemical properties between the catalytic zinc sites of tumor necrosis factor- α -converting enzyme and matrix metalloproteinases despite their high structural similarity. *J. Biol. Chem.* **2004**, *279*, 31646–31654.
- (47) Kevorkian, L.; Young, D. A.; Darrah, C.; Donell, S. T.; Shepstone, L.; Porter, S.; Brockbank, S. M.; Edwards, D. R.; Parker, A. E.; Clark, I. M. Expression profiling of metalloproteinases and their inhibitors in cartilage. *Arthritis Rheum.* **2004**, *50*, 131–141.
- (48) Itoh, T.; Matsuda, H.; Tanioka, M.; Kuwabara, K.; Itohara, S.; Suzuki, R. The role of matrix metalloproteinase-2 and matrix metalloproteinase-9 in antibody induced arthritis. *J. Immunol.* **2002**, *169*, 2643–2647.
- (49) Knight, C. G.; Willenbrock, F.; Murphy, G. A novel coumarin-labelled peptide for sensitive continuous assays of the matrix metalloproteinases. *FEBS Lett.* **1992**, *296*, 263–266.
- (50) SoftMax Pro 4.7.1 by Molecular Devices.
- (51) GraFit version 4 by Erithecus Software.
- (52) Welgus, H. G.; Jeffrey, J. J.; Eisen, A. Z. Human skin fibroblast collagenase. Assessment of activation energy and deuterium isotope effect with collagenous substrates. *J. Biol. Chem.* **1981**, *256*, 9516–9521.
- (53) Bergman, I.; Loxley, R. Lung tissue hydrolysates: studies of the optimum conditions for the spectrophotometric determination of hydroxyproline. *Analyst* **1969**, *94*, 575–584.
- (54) Huey, R.; Morris, G. M.; Olson, A. J.; Goodsell, D. S. A semi-empirical free energy force field with charge-based desolvation. *J. Comput. Chem.* **2007**, *28*, 1145–1152.
- (55) Schuttelkopf, A. W.; van Aalten, D. M. PRODRG: a tool for high-throughput crystallography of protein–ligand complexes. *Acta Crystallogr., Sect. D: Biol. Crystallogr.* **2004**, *60*, 1355–1363.
- (56) Cross, J. B.; Duca, J. S.; Kaminski, J. J.; Madison, V. S. The Active Site of a Zinc-Dependent Metalloproteinase Influences the Computed pK_a of Ligands Coordinated to the Catalytic Zinc Ion. *J. Am. Chem. Soc.* **2002**, *124*, 11004–11007.
- (57) Frisch, M. J.; Trucks, G. W.; Schlegel, H. B.; Scuseria, G. E.; Robb, M. A.; Cheeseman, J. R.; Montgomery, J. A., Jr.; Vreven, T.; Kudin, K. N.; Burant, J. C.; Millam, J. M.; Iyengar, S. S.; Tomasi, J.; Barone, V.; Mennucci, B.; Cossi, M.; Scalmani, G.; Rega, N.; Petersson, G. A.; Nakatsuji, H.; Hada, M.; Ehara, M.; Toyota, K.; Fukuda, R.; Hasegawa, J.; Ishida, M.; Nakajima, T.; Honda, Y.; Kitao, O.; Nakai, H.; Klene, M.; Li, X.; Knox, J. E.; Hratchian, H. P.; Cross, J. B.; Bakken, V.; Adamo, C.; Jaramillo, J.; Gomperts, R.; Stratmann, R. E.; Yazyev, O.; Austin, A. J.; Cammi, R.; Pomelli, C.; Ochterski, J. W.; Ayala, P. Y.; Morokuma, K.; Voth, G. A.; Salvador, P.; Dannenberg, J. J.; Zakrzewski, V. G.; Dapprich, S.; Daniels, A. D.; Strain, M. C.; Farkas, O.; Malick, D. K.; Rabuck, A. D.; Raghavachari, K.; Foresman, J. B.; Ortiz, J. V.; Cui, Q.; Baboul, A. G.; Clifford, S.; Cioslowski, J.; Stefanov, B. B.; Liu, G.; Liashenko, A.; Piskorz, P.; Komaromi, I.; Martin, R. L.; Fox, D. J.; Keith, T.; Al-Laham, M. A.; Peng, C. Y.; Nanayakkara, A.; Challacombe, M.; Gill, P. M. W.; Johnson, B.; Chen, W.; Wong, M. W.; Gonzalez, C.; Pople, J. A. Gaussian 03; Gaussian, Inc.: Pittsburgh, PA, 2003.
- (58) Bayly, C. I.; Cieplak, P.; Cornell, W. D.; Kollman, P. A. A well-behaved electrostatic potential based method using charge restraints for determining atom-centered charges: the RESP model. *J. Phys. Chem.* **1993**, *97*, 10269–10280.
- (59) Cornell, W. D.; Cieplak, P.; Bayly, C. I.; Kollman, P. A. Application of RESP charges to calculate conformational energies, hydrogen bond energies, and free energies of solvation. *J. Am. Chem. Soc.* **1993**, *115*, 9620–9631.
- (60) Cheng, F.; Zhang, R.; Luo, X.; Shen, J.; Li, X.; Gu, J.; Zhu, W.; Shen, J.; Sagi, I.; Ji, R.; Chen, K.; Jiang, H. Quantum Chemistry Study on the Interaction of the Exogenous Ligands and the Catalytic Zinc Ion in Matrix Metalloproteinases. *J. Phys. Chem. B* **2002**, *106*, 4552–4559.
- (61) Case, D. A.; Darden, T. E.; Cheatham, T. E. I.; Simmerling, C. L.; Wang, J.; Duke, R. E.; Luo, R.; Merz, K. M.; Wang, B.; Pearlman, D. A.; Crowley, M.; Brozell, S.; Tsui, V.; Gohlke, H.; Mongan, J.; Hornak, V.; Cui, G.; Beroza, P.; Schafmeister, C.; Caldwell, J. W.; Ross, W. S.; Kollman, P. A. AMBER 9; University of California: San Francisco, 2006.
- (62) Jorgensen, W. L.; Chandrasekhar, J.; Madura, J.; Klein, M. L. *J. Chem. Phys.* **1983**, *79*, 926–935.
- (63) (a) Darden, T.; York, D.; Pedersen, L. Particle mesh Ewald: An *O*(*N*) method for Ewald sums in large systems. *J. Chem. Phys.* **1993**, *98*, 10089–10092. (b) Essmann, U.; Perera, L.; Berkowitz, M. L.; Darden, T.; Lee, H.; Pedersen, L. G. A smooth particle mesh Ewald

method. *J. Chem. Phys.* **1995**, *103*, 8577–8593. (c) Sagui, C.; Darden, T. A. In Simulation and Theory of Electrostatic Interactions in Solution; Pratt, L. R., Hummer, G., Eds.; American Institute of Physics: Melville, NY, 1999; pp 104–113. (d) Toukmaji, A.; Sagui, C.; Board, J.; Darden, T. Efficient particle-mesh Ewald based approach to fixed and induced dipolar interactions. *J. Chem. Phys.* **2000**, *113*, 10913–10927.

- (64) Sanner, M. F. Python: A Programming Language for Software Integration and Development. *J. Mol. Graphics Modell.* **1999**, *17*, 57–61.
- (65) Pettersen, E. F.; Goddard, T. D.; Huang, C. C.; Couch, G. S.; Greenblatt, D. M.; Meng, E. C.; Ferrin, T. E. UCSF Chimera—A Visualization System for Exploratory Research and Analysis. *J. Comput. Chem.* **2004**, *25*, 1605–1612.